THE GEOLOGICAL SOCIETY OF AMERICA®

Rapid cooling history of a Neotethyan ophiolite: Evidence for contemporaneous subduction initiation and metamorphic sole formation

Osman Parlak[1,2,†], István Dunkl[3], Fatih Karaoğlan[1], Timothy M. Kusky[2,4], Chao Zhang[5], Lu Wang[2], Jürgen Koepke[5], Zeki Billor[6], Willis E. Hames[6], Emrah Şimşek[1], Gökçe Şimşek[1], Tuğçe Şimşek[1], and Selena Ezgi Öztürk[1]

[1]*Department of Geological Engineering, Çukurova University, 01330 Balcalı, Adana, Turkey*
[2]*State Key Laboratory of Geological Processes and Mineral Resources, Center for Global Tectonics, School of Earth Sciences, China University of Geosciences, Wuhan 430074, China*
[3]*Geoscience Center, University of Göttingen, Goldschmidtstrasse 3, 37077 Göttingen, Germany*
[4]*Department of Geological Engineering, Middle East Technical University, 06800 Ankara, Turkey*
[5]*Institut für Mineralogie, University of Hannover, Callinstrasse 3, 30167 Hannover, Germany*
[6]*Department of Geology and Geography, Auburn University, Auburn, Alabama 36849, USA*

ABSTRACT

The Beyşehir-Hoyran Nappes, including Mesozoic carbonate platform rocks, deep-sea sediments, and ophiolite-related units, crop out extensively on the western limb of the Isparta Angle in the Central Taurides, Turkey. The ophiolite-related rocks are represented by variably serpentinized harzburgitic mantle tectonites, tectonically underlain by a subophiolitic metamorphic sole and mélange. The harzburgitic mantle tectonites and metamorphic sole are intruded by undeformed isolated dikes. Protoliths of the metamorphic sole are similar to within-plate alkali basalts and associated sediments. The isolated dikes were geochemically derived mainly from tholeiitic magma and, to a lesser extent, from alkaline magma. Five isolated dike samples yielded U-Pb ages ranging from 90.8 ± 1.6 Ma to 87.6 ± 2.1 Ma (zircon) and from 102.3 ± 7.4 Ma to 87.5 ± 7.9 Ma (titanite). Seven amphibolite samples yielded U-Pb age ranges of 91.1 ± 2.1–88.85 ± 1.0 Ma (zircon) and 94.0 ± 4.8–90.0 ± 9.4 Ma (titanite) and a ^{40}Ar-^{39}Ar age range of 93.7 ± 0.3–91.4 ± 0.4 Ma (hornblende). U-Pb and ^{40}Ar-^{39}Ar ages of mineral phases with different closure temperatures (~900–500 °C) from the isolated dikes and metamorphic sole rocks are almost identical and overlapping within 1σ, suggesting that both the magmatic growth of oceanic crust and formation of metamorphic sole were contemporaneous and cooled very rapidly. Hence, all the data should be interpreted as the crystallization ages of the ophiolite and metamorphic sole pair. Genesis of suprasubduction zone–type oceanic crust, genesis and exhumation of the metamorphic sole, and postmetamorphic dike emplacement within the Inner Tauride Ocean can be best explained by subduction initiation and rollback processes during the Late Cretaceous based on petrological and geochronological data obtained from the ophiolitic rocks of the Beyşehir-Hoyran Nappes.

INTRODUCTION

Many Tethyan ophiolites are structurally underlain by thin sheets of metamorphic sole rocks (e.g., Williams and Smyth, 1973; Spray, 1984; Jamieson, 1986; Parlak et al., 1995a; Dilek et al., 1999; Robertson, 2002, 2004). Metamorphic soles are thought to form at the inception of oceanic subduction beneath the hot subophiolitic mantle of the hanging wall (Jamieson, 1986; Malpas, 1979; Spray, 1984; Williams and Smyth, 1973). Initiation of subduction and formation of metamorphic soles have been linked to the ophiolite emplacement process (e.g., Hacker et al., 1996; Jamieson, 1980, 1986; Malpas, 1979; Williams and Smyth, 1973). Because metamorphic soles record hot ophiolite emplacement over cold oceanic crust and associated sediments, it is important to note that the protoliths of the metamorphic soles provide evidence of the nature and composition of former ocean basins (Robertson, 2004).

The spatial and temporal relations of ophiolites and metamorphic soles in the Tethyan realm can be elucidated from Ar-Ar and U-Pb geochronology and geochemistry of crustal rocks and underlying amphibolites. Based on this, metamorphic soles have been interpreted to have formed either (1) during intra-oceanic thrusting shortly after ophiolite formation at mid-ocean ridges (Fig. 1A; Boudier et al., 1988; Hacker, 1994), or (2) during intra-oceanic subduction coeval with ophiolite genesis in suprasubduction zones (Fig. 1B; Pearce et al., 1981; Searle and Malpas, 1980, 1982; Searle and Cox, 2002). The different blocking temperatures of the U-Pb and Ar-Ar systems (Hacker and Gnos, 1997; Spray, 1984) and different cooling histories impeded understanding of the processes in terms of genesis, exhumation, and emplacement of ophiolite and metamorphic sole pairs for many years. Eventually, Warren et al. (2005) were able to date zircons from a metamorphic sole (94.48 ± 0.23 Ma) and trondhjemite (95.3 ± 0.2 Ma) of the Oman ophiolite using the thermal ionization mass spectrometry (TIMS) U-Pb technique and concluded that high-temperature metamorphism during ophiolite emplacement occurred contemporaneously with crystallization of ophiolite crustal differentiates. They suggested a suprasubduction zone origin rather than mid-ocean-ridge origin for the genesis of the Semail ophiolite. Similarly, Rioux et al. (2012, 2013, 2016) and Roberts et al. (2016) reported U-Pb dating results for the crustal rocks and metamorphic sole of the Oman ophiolite. They concluded that the metamorphic sole formed either prior to or during formation of the ophiolite

†parlak@cu.edu.tr

GSA Bulletin; https://doi.org/10.1130/B35040.1; 16 figures; 6 tables; Data Repository item 2019155.

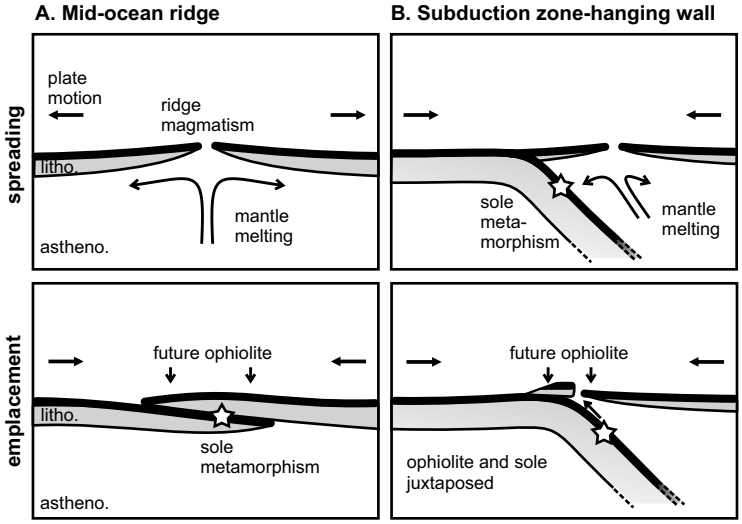

Figure 1. Alternative models for genesis and emplacement of ophiolite and metamorphic soles (from Rioux et al., 2016). Star indicates sites for metamorphic sole; astheno.—asthenosphere, litho.—lithosphere. See text for explanation.

crust, and it was later juxtaposed with the base of the ophiolite.

The ophiolites in northern Turkey are Early to Middle Jurassic in age and interpreted as remnants of the İzmir-Ankara-Erzincan Ocean, which was terminally closed in the Paleocene–Eocene between the Sakarya-Pontide block to the north and the Anatolide-Tauride and Kirşehir continental blocks to the south (Fig. 2; Okay and Tüysüz, 1999; Dilek and Thy, 2006; Çelik et al., 2011; Robertson et al., 2013). In contrast, the ophiolites along the Tauride Mountains in southern Turkey (Lycian Nappes, Antalya, Beyşehir-Hoyran Nappes, Mersin, Pozantı-Karsantı, Pınarbaşı, and Divriği) were emplaced toward the south onto the passive margin of the Tauride carbonate platform during the Late Cretaceous from different Neotethyan oceanic basins (Fig. 2). The Tauride ophiolites have been interpreted as good candidates with which to examine the spatial and temporal relations of

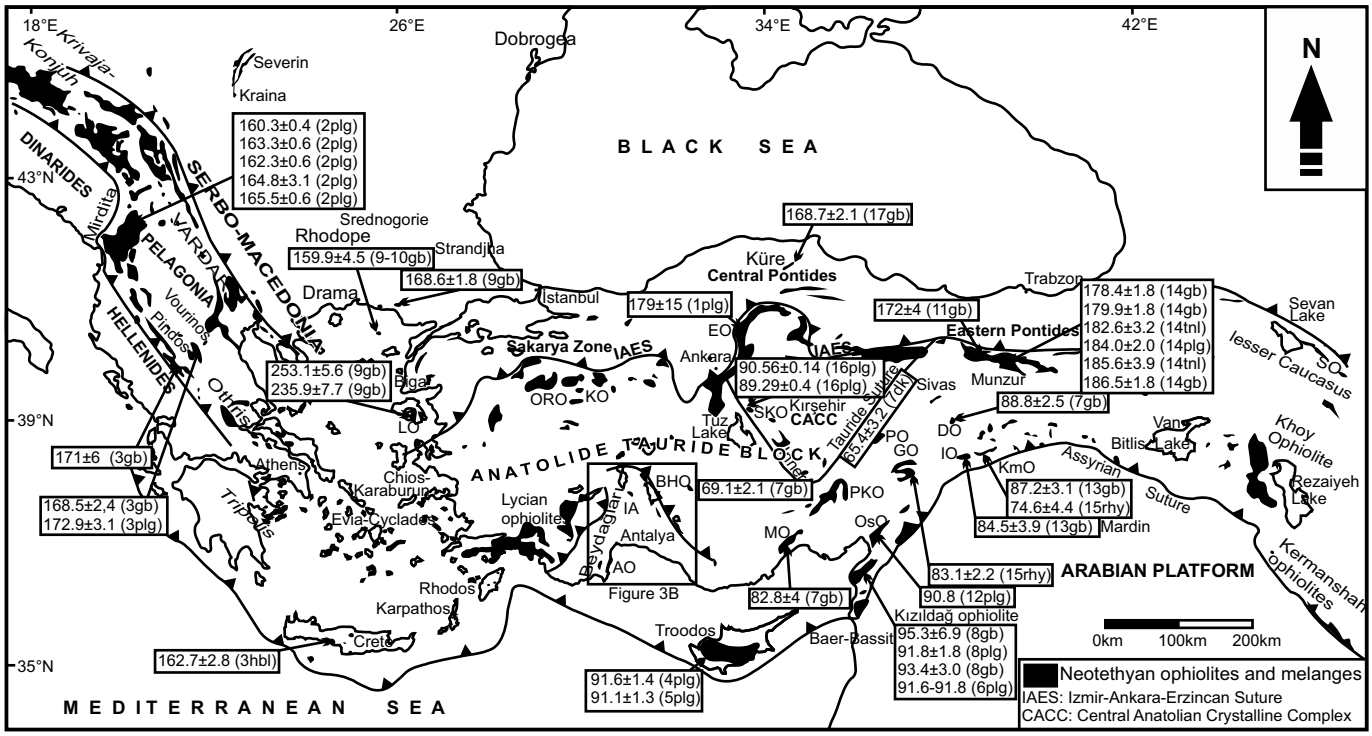

Figure 2. Distribution of the Tethyan ophiolitic formations along the Dinarides, Hellenides, and in Asia Minor. U-Pb ages were compiled from along the entire belt and are presented in the boxes. Red box indicates the study area. Data are from (1) Dilek and Thy (2006), (2) Dilek et al. (2008), (3) Liati et al. (2004), (4) Mukasa and Ludden (1987), (5) Konstantinou et al. (2007), (6) Dilek and Thy (2009), (7) Parlak et al. (2013a), (8) Karaoğlan et al. (2013a), (9) Koglin (2008), (10) Koglin et al. (2009), (11) Topuz et al. (2013), (12) Sarıfakıoğlu et al. (2012), (13) Karaoğlan et al. (2012), (14) Robertson et al. (2013), (15) Karaoğlan et al. (2013b), (16) van Hinsbergen et al. (2016), (17) Alparslan and Dilek (2018). Abbreviations: IA—Isparta Angle, LO—Lesvos ophiolite, AO—Antalya ophiolite, BHO—Beyşehir-Hoyran ophiolite, ORO—Orhaneli ophiolite, KO—Kımık ophiolite, EO—Eldivan ophiolite, MO—Mersin ophiolite, PKO—Pozantı-Karsantı ophiolite; OsO—Osmaniye ophiolite, GO—Göksun (Kahramanmaraş) ophiolite, PO—Pınarbaşı ophiolite, IO—Ispendere ophiolite, DO—Divriği ophiolite, KmO—Kömürhan ophiolite, SO—Sevan ophiolite, SKO—Sarıkaraman ophiolite; plg—plagiogranite, gb—gabbro, hbl—hornblendite, dk—dike, tnl—tonalite, rhy—rhyolite. Base map was modified after Dilek and Flower (2003) and Çelik et al. (2011). The square represents the outline of Figure 3B.

ophiolites and metamorphic soles (Parlak and Delaloye, 1999; Dilek et al., 1999; Robertson, 2004; Çelik et al., 2006; Parlak, 2016).

The Beyşehir-Hoyran Nappes, including Mesozoic carbonate platform deposits, deep-sea sediments, and ophiolite-related units, crop out on the eastern limb of the Isparta Angle in the in Central Taurides, southern Turkey (Fig. 3; Andrew and Robertson, 2002; Monod, 1977; Özgül, 1984; Özgül and Arpat, 1973). The ophiolitic rocks in the Beyşehir-Hoyran Nappes were formed above a north-dipping intra-oceanic subduction zone in the Late Cretaceous, derived from the Inner Tauride Ocean (Andrew and Robertson, 2002; Elitok and Drüppel, 2008). The ophiolite-related rocks are characterized by three main tectonic units, in an ascending order, ophiolitic mélange, subophiolitic metamorphic

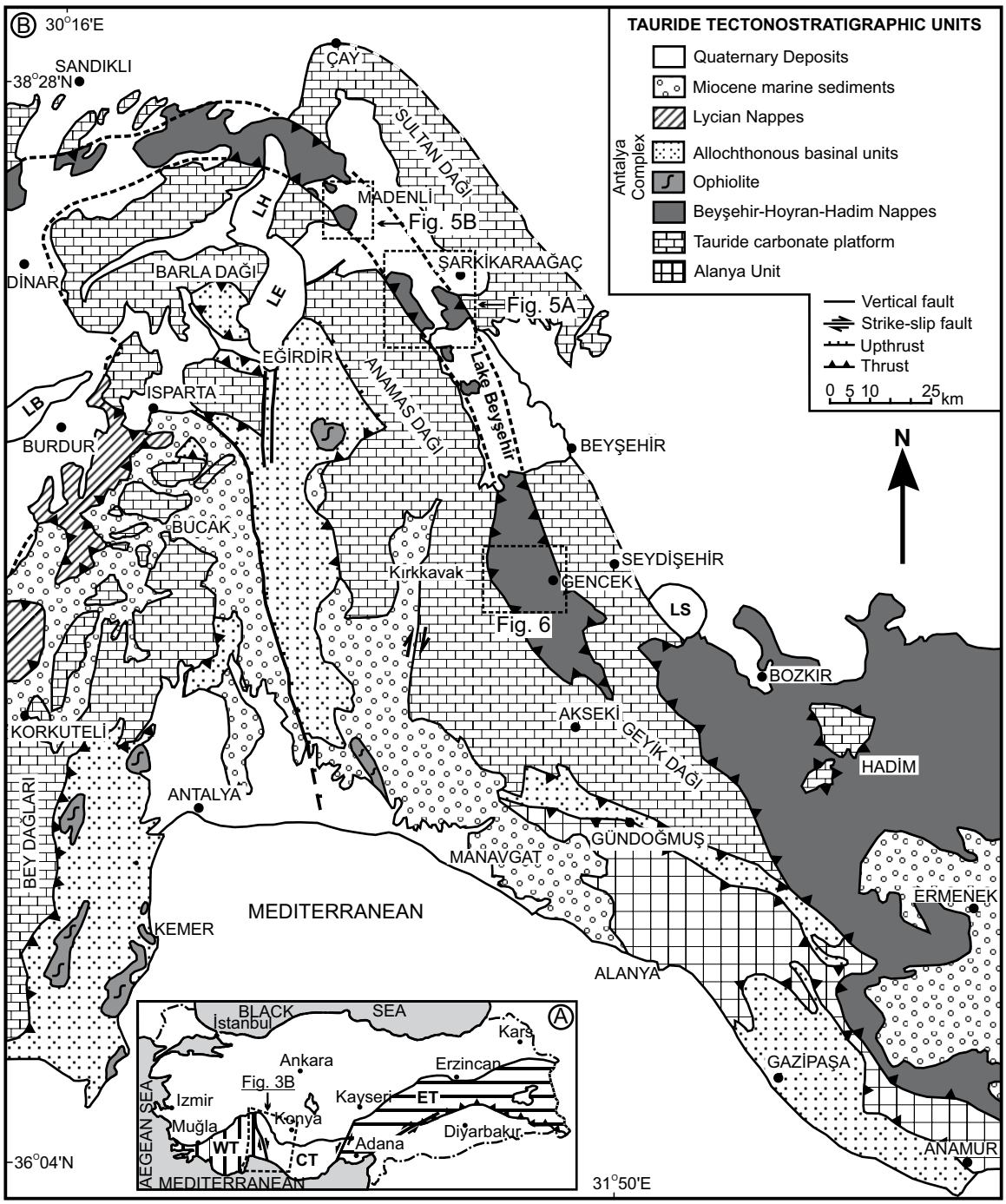

Figure 3. (A) Geographical subdivision of the Tauride belt. Abbreviations, WT—western Taurides, CT—Central Taurides, ET—Eastern Taurides. (B) Distribution of tectonostratigraphic units in the area between Western and Central Taurides (simplified from Özgül, 1984; Andrew and Robertson, 2002). Locations of the Figures 5 and 6 are indicated. Abbreviations: LS—Lake Suğlu, LB—Lake Burdur, LE—Lake Eğirdir, LH—Lake Hoyran.

sole, and oceanic lithospheric remnants (Fig. 4). The plutonic section and the metamorphic sole of the Beyşehir-Hoyran ophiolite are crosscut by numerous postmetamorphic/undeformed, isolated diabase dikes at different structural levels. The only available geochronological data from the Beyşehir-Hoyran ophiolite are based on K-Ar ages (96 ± 3–86 ± 3 Ma) and $^{40}Ar/^{39}Ar$ ages (91.5 ± 1.9–90.9 ± 1.3 Ma) from the metamorphic sole rocks (Çelik et al., 2006; Thuizat et al., 1981).

In this paper, we present zircon and titanite U-Pb laser ablation–sector field–inductively coupled plasma–mass spectrometry (LA-SF-ICP-MS) and hornblende $^{40}Ar/^{39}Ar$ ages and whole-rock and mineral chemistry data for the metamorphic sole and crustal rocks from the Beyşehir-Hoyran ophiolite in the Central Taurides to: (1) better understand the crystallization age and the cooling history of the metamorphic sole and oceanic crust, (2) better understand the tectonic setting of the metamorphic sole and the oceanic crustal rocks, (3) test alternative models, and (4) decipher spatial and temporal relationships between magmatism and deformation within the regional Tethyan framework.

GEOLOGICAL SETTING

The Beyşehir-Hoyran-Hadim Nappes crop out on the eastern limb of the Isparta Angle in the Central Taurides, Turkey (Andrew and Robertson, 2002; Monod, 1977; Özgül, 1984; Özgül and Arpat, 1973). The Isparta Angle is considered to be the site of regional overthrusting of nappes, of dissimilar age and origin, onto the Tauride Platform (Özgül, 1976; Poisson, 1977; Gutnic et al., 1979; Ricou et al., 1979; Koçyiğit, 1984; Morris and Robertson, 1993; Poisson et al., 2003; Robertson et al., 2003). The angular geometry has been interpreted as the result of interference between SE- and SW-verging allochthonous units emplaced during culminating stages of Tethyan convergence between late Campanian and late Miocene times (Gutnic et al., 1979; Poisson et al., 2003; Robertson et al., 2003). Based on origins and emplacement ages, there are three major nappes, namely, (1) the Antalya Complex, (2) the Beyşehir-Hoyran Nappes, and (3) the Lycian Nappes (Fig. 3).

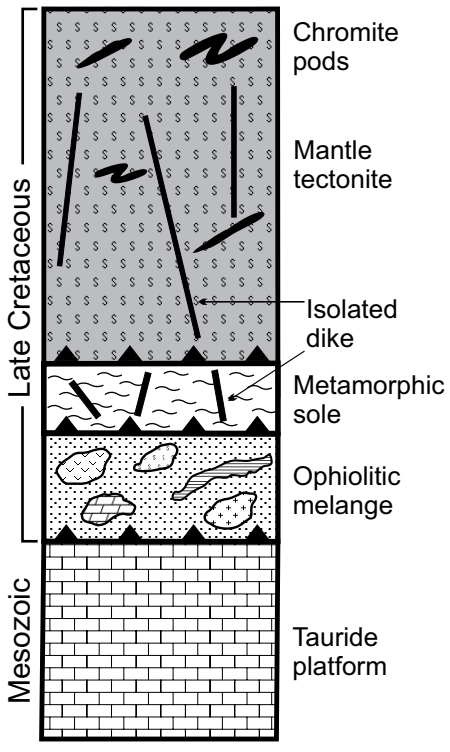

Figure 4. Tectonostratigraphy of the ophiolite-related units in Beyşehir-Hoyran Nappes.

The ophiolite-related rock assemblages are well exposed both to the north and south of Lake Beyşehir (Fig. 3). In the northern part of the Lake Beyşehir area, the ophiolitic rocks are seen at two localities, namely, Şarkikaraağaç and Madenli (Isparta; Fig. 3).

The ophiolitic rocks in the Şarkikaraağaç area tectonically overlie the Tauride carbonate platform to the east (Sultandağ) and to the west (Anamasdağ). These two sides form the limbs of the folded Tauride platform, and Neogene to Quaternary sediments unconformably overlie both the ophiolite and the platform carbonates (Fig. 5A). On the western limb of the folded Tauride platform (Anamasdağ), the ophiolite-related rocks are represented by harzburgitic mantle tectonites at the top, underlain by sub-ophiolitic metamorphic sole and mélange downward (Fig. 5A). Isolated diabase dikes with island-arc geochemistry intrude the mantle tectonites (Elitok and Drüppel, 2008). A thin sheet of highly deformed metamorphic sole rocks with alkaline within-plate and island-arc tholeiite geochemistry, up to 140 m thick, tectonically underlies the harzburgitic mantle tectonites (Elitok and Drüppel, 2008). The metamorphic sole is also cut by postmetamorphic isolated diabase dikes. The ophiolitic mélange comprises blocks of recrystallized limestone, gabbro, isolated diabase, radiolarite, cherts, and siliciclastic rocks set in a strongly sheared serpentinite matrix (Elitok and Drüppel, 2008). The ophiolite-related units in both areas are overthrust by Upper Triassic neritic limestone blocks and large-scale chaotic slope-basin deposits. The limestone unit is known as the Gencek unit (Monod, 1977) in the Central Taurides. On the eastern limb of the folded Tauride platform (Sultandağ), relatively fresh harzburgitic mantle tectonites with minor pyroxenite veins tectonically rest on the autochthonous basement. The harzburgites are intruded by isolated diabase dikes with island-arc tholeiite geochemistry at different structural levels (Elitok and Drüppel, 2008). In the Şarkikaraağaç region, the ophiolites and related units were rethrusted over the Middle Eocene sediments, following the initial Late Cretaceous ophiolite emplacement onto the Tauride platform (Fig. 5A; Mackintosh and Robertson, 2013).

In the Madenli area, the allochthonous units are exposed, namely, metamorphic sole rocks, mantle tectonites, the massive neritic limestone (Gencek unit), and large-scale chaotic slope-basin deposits (Fig. 5B). The metamorphic sole rocks beneath the mantle tectonites are highly deformed and consist mainly of amphibolites. They are intruded by isolated diabase dikes. The strongly sheared and serpentinized harzburgites rest tectonically on the metamorphic sole and are in turn tectonically overlain by the Upper Triassic neritic limestones (Gencek unit) and large-scale chaotic slope-basin deposits (Andrew and Robertson, 2002; Monod, 1977), similar to the Şarkikaraağaç area.

In the southern part of the Lake Beyşehir area (Fig. 3), the ophiolite-related rock assemblages are exposed as thrust slices between the Hadim nappe and the Gencek unit around the town of Gencek (Fig. 6). The ophiolitic mélange unit consists mainly of blocks and fragments of radiolarian cherts, serpentinite, limestone, volcanic rocks, volcaniclastic sediments, serpentinized peridotite, and amphibolites set in a sandstone or mudstone matrix (Andrew and Robertson, 2002). The geochemistry of the volcanic rocks within the mélange exhibits two different compositional trends, including within-plate alkaline basalts and island-arc tholeiitic basalts (Andrew and Robertson, 2002). Protoliths of the metamorphic sole amphibolites are more akin to within-plate alkaline basalt (Çelik and Delaloye, 2006). The peridotite body in the mélange is represented by serpentinized harzburgite and dunite intruded by numerous isolated diabase dikes at different structural levels. The ages of the units within the mélange range from Triassic to Late Cretaceous. The ophiolitic mélange has been interpreted as a subduction-accretion complex, with final emplacement onto the Tauride platform ending by the Maastrichtian (Andrew and Robertson, 2002).

ANALYTICAL METHODS

To determine the geochemical and petrological characteristics of the isolated diabase dikes and amphibolites from the metamorphic sole, 16 samples were analyzed for whole-rock major and trace elements (including rare earths). Two isolated dike samples and four

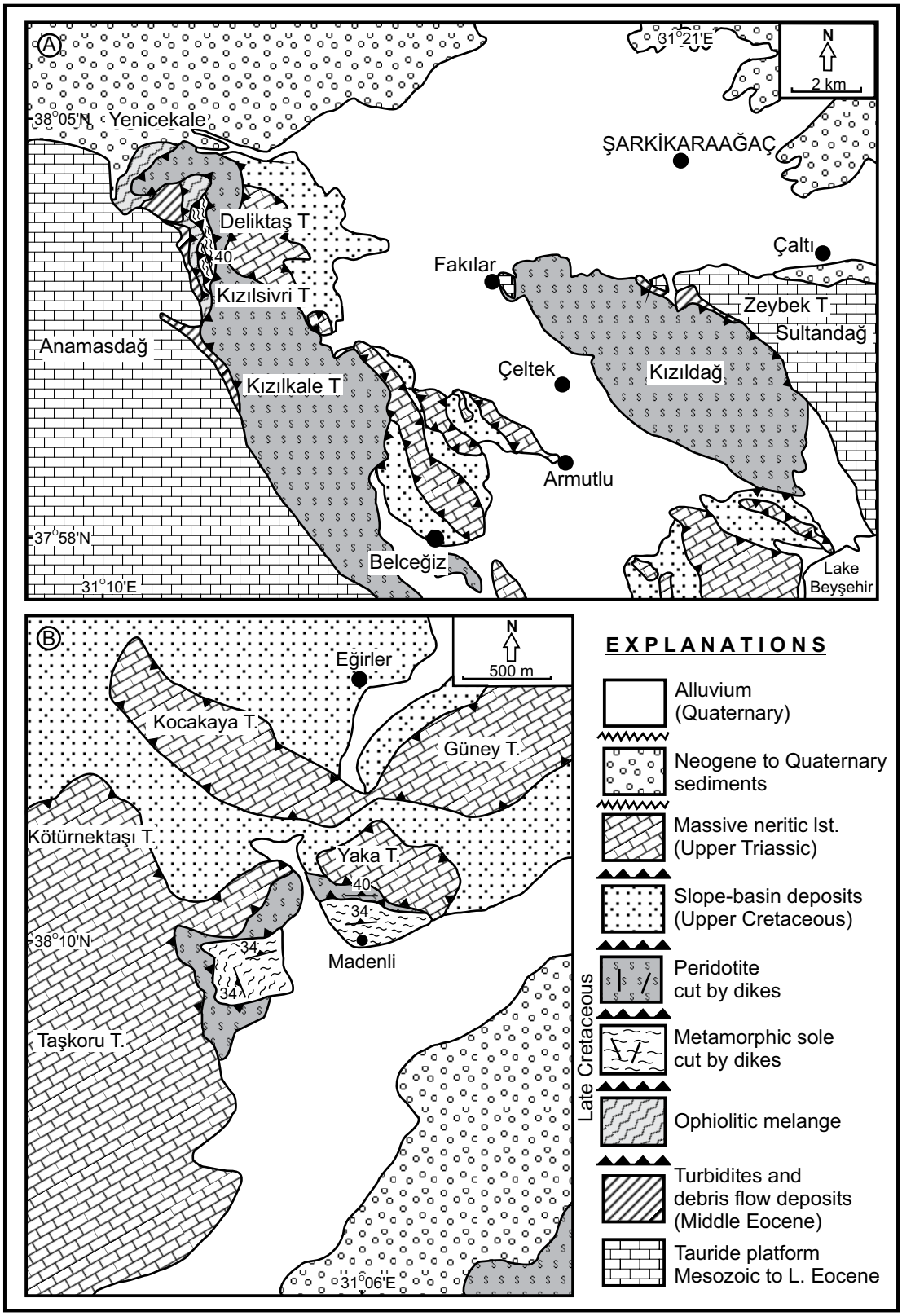

Figure 5. (A) Geological map of the Şarkikaraağaç area (from Elitok and Drüppel, 2008). (B) Geological map of the Madenli area (from Elitok and Drüppel, 2008). Abbreviations: lst.—limestone; L.—Lower; T.—Tepe.

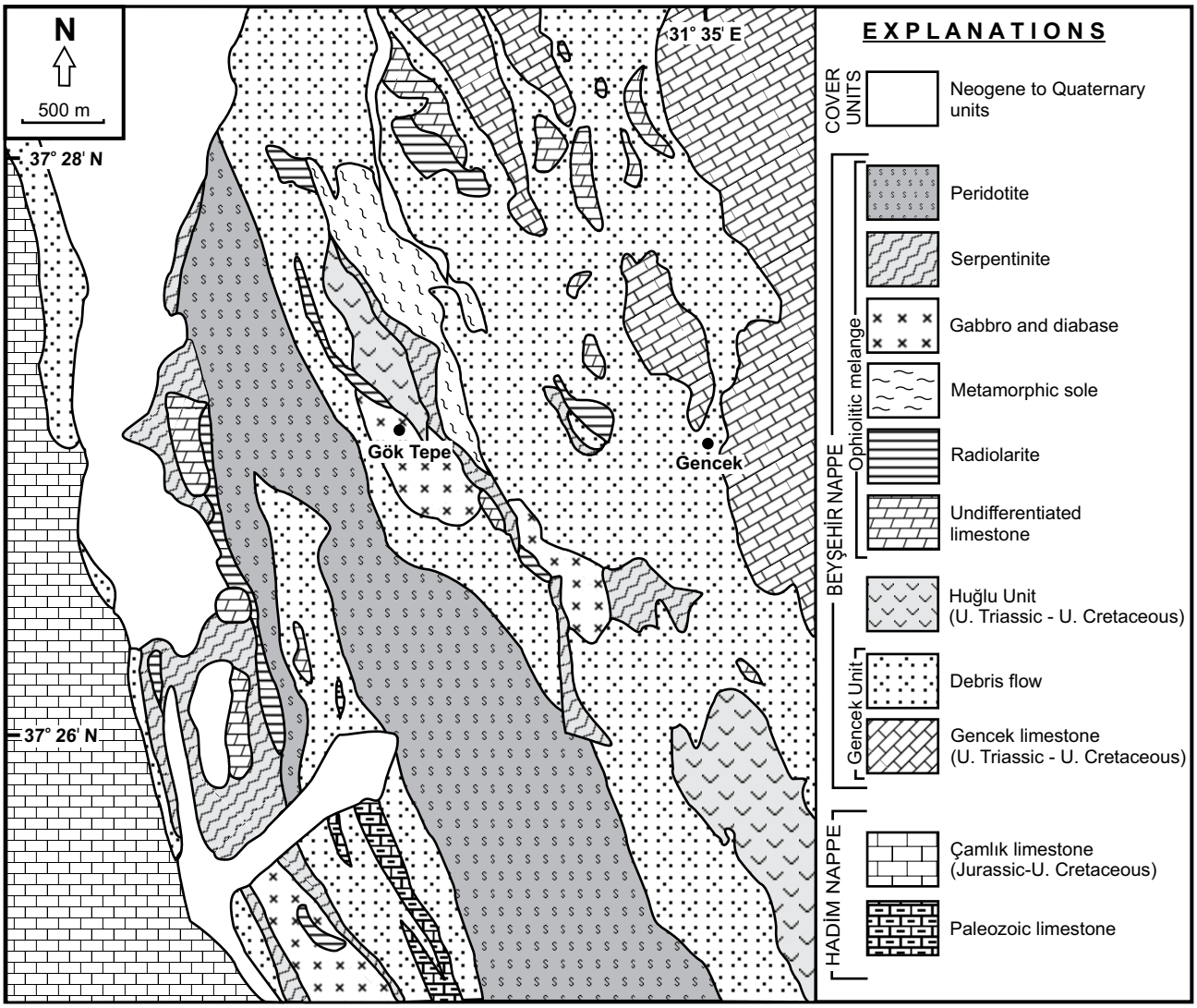

Figure 6. Simplified geological map of the Gencek (Konya) area (from Monod, 1977); U.—Upper.

metamorphic sole samples were analyzed at Acme Analytical Laboratories, Ltd. (Canada). Major-element contents were determined from a $LiBO_2$ fusion by inductively coupled plasma–emission spectrometry (ICP-ES) by using 5 g of sample pulp. Trace-element contents were determined from a $LiBO_2$ fusion by inductively coupled plasma–mass spectrometry (ICP-MS) by using 5 g of sample pulp. Major- and trace-element contents of four isolated dikes and six metamorphic sole samples were analyzed at the State Key Laboratory for Geological Processes and Mineral Resources, China University of Geosciences, Wuhan, China. Whole-rock major-element compositions were measured using a Shimadzu XRF-1800 sequential X-ray fluorescence spectrometer, with the detailed experimental processes and conditions described by Ma et al. (2012). Whole-rock trace elements were analyzed using an Agilent 7500a ICP-MS, with the detailed sample-digestion procedure for ICP-MS analyses, analytical precision, and accuracy for trace elements including rare earth, high field strength, and large ion lithophile elements, and transition metals following the protocols of Liu et al. (2008). About 50 mg samples were digested by HF + HNO_3 in Teflon bombs for ICP-MS analysis. Sample dissolution was conducted under superclean laboratory conditions. International standards AGV-2, BHVO-2, and RGM-2 were used as reference materials to estimate analytical precision. The results of the analyses are presented in Tables 1 and 2.

Electron microprobe analysis was carried out on eight representative polished sections of the metamorphic sole rocks using a CAMECA SX-100 instrument at the Institute of Mineralogy, Leibniz University, Hannover, Germany. The analytical conditions for the elements were 10–30 s counting interval, a beam current of 15 nA, and an acceleration voltage of 15 kV. Raw data were revised by a PAP matrix correction (Pouchou and Pichoir, 1984). The representative results are presented in Tables 3, 4, and 5.

Cathodoluminescence (CL) images were produced using a Zeiss Supra 55 scanning electron microscope (SEM) at the central laboratory of Mersin University, Mersin, Turkey. CL photos of the zircons from the dated samples are provided as Supplementary Files 1–3.[1]

[1]GSA Data Repository item 2019155, Supplementary Files 1–6, cathodoluminescence photos and analytical data, is available at http://www.geosociety.org/datarepository/2019 or by request to editing@geosociety.org.

TABLE 1. MAJOR- AND TRACE-ELEMENT CONTENTS OF THE METAMORPHIC SOLE ROCKS FROM THE BEYŞEHIR-HOYRAN OPHIOLITE

	Metamorphic sole									
	Şarkikaraağaç						Gencek			
Sample no.:	S14-1	S14-3	S14-4	S14-5	S15-1†	S15-3†	G14-1	G14-4	G15-3†	G15-4†
Major oxides (wt%)										
SiO_2	45.84	39.46	44.32	45.48	45.94	38.74	45.22	43.55	42.48	45.84
TiO_2	2.24	2.52	2.7	2.39	2.88	2.94	2.32	2.89	3.44	2.68
Al_2O_3	10.71	10.55	9.07	11.06	11.10	10.39	9.93	12.99	10.73	12.89
FeO*	12.69	11	17.75	13.01	13.57	11.88	13.28	14.75	14.10	12.61
MnO	0.16	0.17	0.48	0.17	0.19	0.17	0.16	0.17	0.19	0.17
MgO	11.67	7.12	10.92	13.72	9.81	7.31	12.86	9.1	12.62	9.21
CaO	12	16.57	10.7	8.73	9.94	18.10	11.92	10.73	10.97	9.02
Na_2O	1.82	2.64	1.28	2.49	2.98	2.10	1.69	1.95	2.17	3.40
K_2O	0.77	1.33	0.79	0.98	0.79	1.54	0.52	1.71	0.66	1.68
P_2O_5	0.29	0.33	0.4	0.34	0.57	0.58	0.26	0.33	0.48	0.41
Cr_2O_3	na	na	na	na	0.057	0.035	na	na	0.106	0.056
LOI	1.99	7.96	1.19	1.59	1.8	5.8	1.52	1.87	1.6	1.5
TOT/C	na	na	na	na	<0.02	1.44	na	na	0.03	0.02
TOT/S	na	na	na	na	<0.02	<0.02	na	na	<0.02	<0.02
Total	100.18	99.65	99.6	99.96	99.65	99.67	99.68	100.04	99.64	99.64
Trace elements (ppm)										
Sc	27.2	30.0	49.4	27.2	27	20	26.8	34.7	31	24
V	224	229	269	253	293	255	215	307	269	258
Cr	626	488	408	615	na	na	906	305	na	na
Co	59.9	46.3	84.3	60.1	50.9	45.9	66.8	51.9	71.0	53.3
Ni	398	191	270	400	165	122	511	156	404	223
Ga	15.8	16.5	19.3	17.3	19.2	18.2	16.2	19.3	16.4	16.8
Rb	11.1	22.1	8.34	16.2	8.0	20.4	4.30	31.7	6.2	26.7
Sr	284	325	76.1	398	374.1	641.4	178	496	330.9	704.9
Y	22.0	22.3	92.6	24.5	30.5	26.0	21.8	27.6	23.4	24.6
Zr	167	190	207	183	273.3	265.9	152	143	171.6	229.1
Nb	37.8	36.0	89.0	36.8	52.4	58.4	25.5	31.5	41.6	42.5
Cs	0.095	0.25	0.087	0.16	0.2	<0.1	0.042	0.24	<0.1	0.1
Ba	221	150	80.9	298	343	702	90.8	454	268	1358
Hf	4.05	4.63	5.81	4.46	6.4	6.3	3.93	3.73	4.6	5.4
Ta	2.28	2.22	7.47	2.24	3.6	3.2	1.60	1.91	2.8	2.5
Pb	1.60	1.81	3.13	1.92	na	na	1.38	1.03	na	na
Th	2.99	2.47	11.8	2.81	4.2	5.3	3.27	1.92	2.5	3.6
U	1.33	0.74	1.99	0.69	1.5	1.2	0.75	0.51	0.7	0.8
La	27.6	24.0	74.8	27.3	46.8	52.0	22.7	21.3	30.3	38.0
Ce	55.5	52.6	183	58.0	100.2	97.9	48.1	48.6	62.0	75.2
Pr	6.85	6.75	21.7	7.19	12.98	11.80	5.94	6.32	7.94	9.41
Nd	27.4	28.7	90.5	29.8	53.1	47.6	24.7	27.0	32.8	37.3
Sm	5.74	6.07	19.6	6.45	10.05	8.62	5.60	6.30	6.54	7.57
Eu	1.89	1.99	5.26	2.14	3.18	2.66	1.91	2.22	2.17	2.30
Gd	5.47	5.74	18.0	6.05	9.17	7.72	5.56	6.49	6.20	6.70
Tb	0.79	0.86	2.79	0.91	1.28	1.04	0.82	0.99	0.91	0.97
Dy	4.42	4.62	16.3	4.88	6.54	5.56	4.47	5.59	4.70	5.12
Ho	0.83	0.83	3.13	0.89	1.19	0.96	0.82	0.99	0.88	0.92
Er	2.08	2.09	8.45	2.36	3.03	2.34	2.08	2.56	2.44	2.43
Tm	0.28	0.29	1.17	0.31	0.40	0.29	0.27	0.34	0.29	0.30
Yb	1.75	1.77	7.02	1.88	2.33	1.67	1.64	2.13	1.78	1.76
Lu	0.24	0.24	0.93	0.28	0.32	0.24	0.23	0.29	0.25	0.27

Note: Total Fe is expressed as FeO*; LOI—loss on ignition; < means below detection limit; na—not analyzed; TOT/C—Total carbon; TOT/S—Total sulfur.

†Analyzed at ACME and others at China University of Geosciences in Wuhan.

Zircon crystals were fixed on a double-sided adhesive tape stuck on a thick glass plate and embedded in a 25-mm-diameter epoxy mount. The crystal mounts were lapped by 2500 mesh SiC paper and polished by 9, 3, and 1 µm diamond suspensions. For all zircon samples and standards used in this study, CL images were obtained using a JEOL JXA 8900 electron microprobe at the Geozentrum Göttingen, Göttingen, Germany, in order to study their internal structure and to select homogeneous parts for the in situ age determinations. The in situ U-Pb dating was performed by single-collector LA-SF-ICP-MS. The method employed for analysis was described in detail by Frei and Gerdes (2009). A Thermo Finnigan Element 2 mass spectrometer, coupled to a Resonetics excimer laser ablation system, was used. All age data presented here were obtained by single-spot analyses with a laser beam diameter of 33 µm and a crater depth of ~10 µm. The laser was fired at a repetition rate of 5 Hz and at nominal laser energy output of 25%. Two laser pulses were used for pre-ablation. The carrier gases were He and Ar. Analytes of ^{238}U, ^{235}U, ^{232}Th, ^{208}Pb, ^{207}Pb, ^{206}Pb, mass 204, and ^{202}Hg were measured by the ICP-MS. The data reduction was based on the processing of ~50 selected time slices (corresponding to ~14 s) starting ~3 s after the beginning of the signal. The age calculation and quality control were based on drift and fractionation correction by standard-sample bracketing using GJ-1 zircon reference material (Jackson et al., 2004). For further control, the Plešovice zircon (Sláma et al., 2008), the 91500 zircon (Wiedenbeck et al., 1995), and the FC-1 zircon (Paces and Miller, 1993) were analyzed as "secondary standards." The age results of the standards were consistently within 2σ of the published isotope dilution (ID) TIMS values. Drift and fractionation corrections and data reductions were performed using our in-house software (UranOS; Dunkl et al., 2008). The analytical data for zircon and titanite U-Pb dating are provided as Supplementary Files 4 and 5, respectively (see footnote 1).

The $^{40}Ar/^{39}Ar$ geochronology was carried out on handpicked amphibole grains from amphibolites of the metamorphic sole at the Auburn Noble Isotope Mass Analysis Laboratory (ANIMAL), Auburn University, Auburn, Alabama. Four amphibolite samples were collected for $^{40}Ar/^{39}Ar$ geochronology. The samples were selected on the basis of structural setting and petrography. The four selected amphibolite samples were crushed and sieved (250–180 µm), and hornblende grains were handpicked under a binocular microscope to be free from visible alteration, inclusions, or other phases. The selected samples were washed with deionized water in an ultrasonic cleaner. Around 300 amphibole grains were individually wrapped in domestic Al-foil and placed in an Al-irradiation disk with monitor FC-2 (age = 28.02 Ma; Renne et al., 1998) along with a CaF_2 flux monitor. All samples and standards were irradiated in the U.S. Geological Survey Triga Reactor in Denver, Colorado. The laboratory is equipped with a low-volume, high-sensitivity, 10-cm-radius sector mass spectrometer and automated sample extraction system (50 W Synrad CO_2 laser) for the analysis of samples. The analyses were conducted by incremental heating analysis of 80 hornblende grains from each sample. All of the statistical $^{40}Ar/^{39}Ar$ ages in this study are quoted at the 95% confidence

TABLE 2. MAJOR- AND TRACE-ELEMENT CONTENTS OF THE ISOLATED DIKE ROCKS FROM THE BEYŞEHIR-HOYRAN NAPPES

	Isolated dikes					
	Şarkikaraağaç		Gencek			
Sample no.:	S14-2	S15-2†	G14-2	G14-3	G14-5	G15-1†
Major oxides (wt%)						
SiO_2	48.46	46.85	48.59	50.37	50.13	49.63
TiO_2	1.09	3.05	1.08	1.2	0.71	0.86
Al_2O_3	14.23	12.55	15.14	14.85	14.42	16.07
FeO*	10.27	12.67	10.23	11.06	9.76	9.10
MnO	0.16	0.17	0.16	0.17	0.14	0.14
MgO	7.46	8.81	7.21	6.83	5.86	6.44
CaO	10.39	8.16	10.32	9.36	9.12	8.59
Na_2O	3.22	3.52	3.44	3.29	4.53	4.25
K_2O	0.64	1.01	0.32	0.39	0.28	1.12
P_2O_5	0.08	0.50	0.08	0.08	0.04	0.05
Cr_2O_3	na	0.039	na	na	na	0.015
LOI	3.66	2.3	3.04	2.04	4.63	3.5
TOT/C	na	<0.02	na	na	na	0.04
TOT/S	na	<0.02	na	na	na	0.08
Total	99.66	99.66	99.61	99.64	99.62	99.82
Trace elements (ppm)						
Sc	39.1	26	37.7	38.0	35.5	36
V	274	263	263	303	286	278
Cr	188	na	167	81.6	36.8	na
Co	37.6	44.5	37.7	37.2	32.7	35.4
Ni	68.8	94	93.3	64.2	43.7	56
Ga	14.4	19.0	15.2	16.9	14.0	16.0
Rb	16.8	20.7	4.07	3.95	5.39	16.2
Sr	593	540.6	252	194	64.9	132.2
Y	25.6	26.7	24.0	28.4	19.3	20.9
Zr	60.2	242.4	57.6	65.1	30.8	49.6
Nb	2.19	45.9	1.11	1.19	0.71	0.6
Cs	2.85	0.4	0.35	0.13	0.48	0.2
Ba	354	575	41.2	35.6	24.3	33
Hf	1.75	6.1	1.77	1.95	1.10	1.5
Ta	0.13	3.0	0.073	0.088	0.057	<0.1
Pb	0.87	na	1.49	1.22	0.88	na
Th	0.59	3.8	0.19	0.20	0.13	<0.2
U	0.15	0.9	0.068	0.074	0.079	<0.1
La	5.28	40.0	2.58	2.69	1.23	2.0
Ce	12.3	80.8	7.75	8.21	3.63	6.0
Pr	1.75	10.50	1.29	1.41	0.62	1.02
Nd	8.41	42.5	6.98	7.77	3.50	6.1
Sm	2.68	8.67	2.49	2.80	1.42	2.10
Eu	0.98	2.64	0.95	1.02	0.52	0.90
Gd	3.55	7.61	3.27	3.83	2.22	2.94
Tb	0.66	1.11	0.61	0.70	0.42	0.54
Dy	4.37	5.89	4.02	4.80	3.10	3.64
Ho	0.92	1.05	0.88	0.99	0.66	0.82
Er	2.77	2.66	2.53	2.95	2.08	2.39
Tm	0.40	0.34	0.36	0.44	0.30	0.34
Yb	2.60	2.04	2.44	2.86	2.15	2.17
Lu	0.38	0.28	0.36	0.43	0.34	0.32

Note: Total Fe is expressed as FeO*; LOI—loss on ignition; < means below detection limit; na—not analyzed; TOT/C—Total carbon; TOT/S—Total sulfur.

†Analyzed at ACME and others at China University of Geosciences in Wuhan.

level, whereas errors in individual measurements are quoted as one standard deviation (1σ). Data reduction and assessment of statistical ages were done using Microsoft Excel and Isoplot (Ludwig, 2003). The full data set for the dated samples is provided in Supplementary File 6 (see footnote 1).

PETROGRAPHY AND MINERALOGY

The serpentinized mantle tectonites (harzburgite and dunite) in the Beyşehir-Hoyran Nappes are intruded by numerous isolated dikes (Fig. 7A). The dikes also intruded the metamorphic sole in the region (Fig. 7C). The isolated dikes are petrographically identified as microgabbro to diabase and exhibit subophitic to microgranular porphyritic textures (Fig. 7B). The microgabbro-diabase dikes are 2–7 m in thickness (Fig. 7A). They consist of plagioclase (60%–65%) and clinopyroxene (35%–40%). The clinopyroxenes are present either as occupying spaces between plagioclase laths or as large phenocrysts, and they are partly transformed to amphibole, especially along their rims.

The metamorphic sole rocks in the regions of Gencek (Konya) and Şarkikaraağaç-Madenli (Isparta) include the following rock association: amphibolite, plagioclase amphibolite, plagioclase amphibole schist, and plagioclase-epidote-amphibole schist (Figs. 7C–7F). The metamorphic sole rocks exhibit granoblastic and nematoblastic textures (Figs. 7D–7F). They display well-developed foliation due to the preferred orientation of hornblende and plagioclase (Fig. 7E). Amphibolitic metamorphic soles consist of hornblende-dominated dark layers that alternate with light bands, lenses, and stringers composed of plagioclase and epidote. Amphibole is the most common phase in the metamorphic sole rocks, and it is typically represented by euhedral to subhedral hornblende (60%–95%). The plagioclase (15%–25%) exhibits strong alteration products, including calcite, albite, and sericite. Epidote and chlorite are common in lower-amphibolite- and greenschist-facies rocks of the metamorphic sole. K-feldspar also occurs as veins. Titanite, rutile, zircon, and opaque minerals are the accessory phases. In addition, garnet-amphibolite and pyroxene-amphibolite rock types with granoblastic texture are reported from the metamorphic soles in Gencek (Konya) and Şarkikaraağaç (Isparta) areas (Çelik and Delaloye, 2006; Elitok and Drüppel, 2008).

Based on the amphibole classification of Leake et al. (1997), all analyzed amphiboles are of calcic-type amphiboles (Fig. 8A). In the Gencek area, the amphiboles are characterized by magnesiohastingsite, magnesiohornblende, edenite, pargasite, and tschermakite in a decreasing amounts (Fig. 8A). In the Şarkikaraağaç-Madenli area, the amphiboles are represented by magnesiohornblende, magnesiohastingsite, tschermakite, edenite, actinolite, and ferropargasite in decreasing amounts (Fig. 8A). The amphiboles do not exhibit considerable zoning from cores to rims (Table 3).

Clinopyroxene is present within the metamorphic sole rocks in both the Gencek (Konya) and Şarkikaraağaç-Madenli (Isparta) areas, mainly Ca-rich and diopside in composition ($Wo_{49–57}$; $En_{32–46}$; $Fs_{3–15}$; Fig. 8B).

Feldspars show a large range in composition (Fig. 8C). In the Gencek area, feldspars are generally altered, and they have albite

TABLE 3. REPRESENTATIVE ANALYSES OF MAJOR ELEMENTS FOR THE AMPHIBOLES FROM THE METAMORPHIC SOLE ROCKS

	Gencek (Konya)								Şarkikaraağaç-Madenli (Isparta)							
Sample no.:	G14-1-47	G14-1-49	G14-4-17	G14-4-18	G15-3-17	G15-3-18	G15-4-19	G15-4-20	S14-1-41	S14-1-44	S14-4-22	S14-4-23	S15-1-1	S15-1-2	S15-3-1	S15-3-2
Major oxides/elements (wt%)																
SiO_2	44.79	45.63	42.80	41.69	43.96	43.84	40.78	41.28	45.17	44.42	44.31	43.25	52.62	55.54	40.57	38.31
TiO_2	1.29	1.22	1.50	1.42	1.87	1.86	2.32	1.76	1.20	1.48	0.94	1.23	0.32	0.02	0.80	1.32
Al_2O_3	10.68	9.88	11.16	11.78	11.40	11.10	11.56	11.41	10.68	11.04	10.87	10.89	4.94	1.83	12.47	14.25
FeO*	12.75	11.90	16.26	16.48	12.22	12.43	17.91	18.20	11.87	12.19	15.15	15.57	9.45	7.57	18.28	18.41
MgO	13.64	14.64	0.26	0.32	0.19	0.14	0.15	0.28	13.96	14.35	11.86	11.94	0.23	-0.01	9.85	9.17
MnO	0.09	0.18	10.75	10.59	13.85	14.00	10.16	10.02	0.18	0.15	0.57	0.41	17.65	19.68	0.30	0.19
CaO	11.43	11.64	11.31	11.67	11.18	11.28	11.32	11.43	11.50	11.62	11.08	11.21	12.43	13.15	11.20	11.52
Na_2O	1.98	2.06	2.35	2.41	2.67	2.59	2.26	2.20	2.22	2.02	1.77	1.69	0.40	0.14	2.66	2.61
K_2O	0.52	0.45	0.38	0.43	0.36	0.35	1.29	1.29	0.55	0.59	0.81	0.82	0.09	0.00	1.13	1.53
Fl	0.00	0.00	0.11	0.00	na	na	na	na	0.00	0.00	0.08	0.01	na	na	na	na
Cl	0.00	0.00	0.60	0.56	na	na	na	na	0.00	0.00	0.01	0.00	na	na	na	na
Cr_2O_3	0.08	0.16	0.00	0.13	na	na	na	na	0.01	0.14	0.03	0.05	na	na	na	na
Total	97.26	97.77	97.48	97.48	97.70	97.60	97.74	97.86	97.32	98.01	97.49	97.07	98.13	97.91	97.27	97.30
Si	6.51	6.57	6.40	6.26	6.36	6.35	6.14	6.21	6.56	6.39	6.49	6.37	7.35	7.73	6.13	5.84
Al iv	1.49	1.43	1.60	1.74	1.64	1.65	1.86	1.79	1.44	1.61	1.51	1.63	0.65	0.27	1.87	2.16
Al vi	0.34	0.25	0.37	0.34	0.31	0.25	0.19	0.23	0.38	0.26	0.37	0.27	0.16	0.03	0.34	0.40
Ti	0.14	0.13	0.17	0.16	0.20	0.20	0.26	0.20	0.13	0.16	0.10	0.14	0.03	0.00	0.09	0.15
Cr	0.01	0.02	0.00	0.02	0.00	0.00	0.00	0.00	0.00	0.02	0.00	0.01	0.00	0.00	0.00	0.00
Fe^{3+}	0.65	0.64	0.51	0.52	0.64	0.70	0.59	0.59	0.49	0.76	0.79	0.91	0.58	0.27	0.73	0.63
Fe^{2+}	0.90	0.79	1.52	1.55	0.83	0.81	1.66	1.70	0.95	0.71	1.07	1.01	0.52	0.61	1.58	1.71
Mn	0.01	0.02	0.03	0.04	0.02	0.02	0.02	0.04	0.02	0.02	0.07	0.05	0.03	0.00	0.04	0.02
Mg	2.95	3.14	2.40	2.37	2.99	3.03	2.28	2.25	3.02	3.08	2.59	2.62	3.67	4.08	2.22	2.08
Ca	1.78	1.80	1.81	1.88	1.73	1.75	1.83	1.84	1.79	1.79	1.74	1.77	1.86	1.96	1.81	1.88
Na	0.56	0.58	0.68	0.70	0.75	0.73	0.66	0.64	0.62	0.56	0.50	0.48	0.11	0.04	0.78	0.77
K	0.10	0.08	0.07	0.08	0.07	0.07	0.25	0.25	0.10	0.11	0.15	0.15	0.02	0.00	0.22	0.30
F	0.00	0.00	0.05	0.00	–	–	–	–	0.00	0.00	0.04	0.01	0.00	0.00	-	-
Cl	0.00	0.00	0.15	0.14	–	–	–	–	0.00	0.00	0.00	0.00	0.00	0.00	-	-
Total	15.43	15.45	15.77	15.81	15.55	15.54	15.73	15.73	15.51	15.46	15.43	15.41	14.98	15.00	15.81	15.95
Mg#	0.77	0.80	0.61	0.61	0.78	0.79	0.58	0.57	0.76	0.81	0.71	0.72	0.88	0.87	0.58	0.55

Note: Number of ions is based on 23 oxygens; total Fe is expressed as FeO*; na—not analyzed; – —not calculated.

TABLE 4. REPRESENTATIVE ANALYSES OF MAJOR ELEMENTS FOR THE FELDSPARS FROM THE METAMORPHIC SOLE ROCKS

	Gencek (Konya)							Sarkikaraağaç-Madenli (Isparta)							
Sample no.:	G14-1-38	G14-1-40	G14-4-1	G14-4-9	G15-3-2	G15-3-3	G15-4-1	S14-1-33	S14-1-32	S14-4-1c	S14-4-3	S15-1-2	S15-1-5	S15-3-1	S15-3-2
Major oxides (wt%)															
SiO_2	62.12	64.58	63.79	62.93	64.73	66.79	62.52	67.82	68.41	63.99	62.58	44.89	44.50	65.99	66.49
Al_2O_3	23.11	19.38	19.12	19.69	18.35	22.07	20.53	20.08	20.02	22.77	23.71	34.88	34.99	23.22	20.83
FeO*	0.50	0.08	0.05	0.06	0.11	0.07	0.19	0.10	0.06	0.10	0.00	0.34	0.22	0.18	0.40
MgO	0.26	0.03	0.00	0.00	0.00	0.13	0.02	0.00	0.00	0.00	0.00	na	na	0.04	0.10
CaO	0.82	0.43	0.13	0.09	0.00	1.14	0.06	0.14	0.22	3.62	4.52	18.75	19.05	0.28	0.16
Na_2O	8.67	5.08	0.23	0.32	0.16	10.48	4.33	11.19	11.39	9.57	8.92	0.84	0.91	9.59	5.16
K_2O	3.39	9.01	15.63	15.77	16.36	0.93	10.53	0.30	0.12	0.12	0.10	0.00	0.00	1.99	8.96
Total	98.87	98.59	98.95	98.86	99.70	101.60	98.31	99.64	100.23	100.17	99.83	99.71	99.69	101.27	102.08
Si	2.80	2.96	2.97	2.94	3.00	2.89	2.90	2.97	2.98	2.82	2.77	2.08	2.07	2.87	2.94
Al	1.23	1.05	1.05	1.09	1.00	1.13	1.12	1.04	1.03	1.18	1.24	1.91	1.91	1.19	1.08
Fe	0.02	0.00	0.00	0.00	0.00	0.00	0.01	0.00	0.00	0.00	0.00	0.00	0.00	0.01	0.01
Mg	0.02	0.00	0.00	0.00	0.00	0.01	0.00	0.00	0.00	0.00	0.00	0.01	0.01	0.00	0.01
Ca	0.04	0.02	0.01	0.01	0.00	0.05	0.00	0.01	0.01	0.17	0.21	0.93	0.95	0.01	0.01
Na	0.76	0.45	0.02	0.03	0.01	0.88	0.39	0.95	0.96	0.82	0.77	0.08	0.08	0.81	0.44
K	0.20	0.53	0.93	0.94	0.97	0.05	0.62	0.02	0.01	0.01	0.01	0.00	0.00	0.11	0.50
Total	5.06	5.01	4.98	5.00	4.99	5.01	5.05	4.99	4.99	5.00	5.00	5.01	5.02	5.00	4.99
Or	19.64	52.72	97.15	96.53	98.51	5.21	61.36	1.74	0.70	0.68	0.56	0.01	0.03	11.86	52.93
Ab	76.35	45.18	2.19	2.98	1.49	89.43	38.36	97.59	98.24	82.14	77.69	7.50	7.94	86.74	46.28
An	4.01	2.10	0.66	0.49	0.00	5.36	0.28	0.67	1.05	17.19	21.75	92.48	92.03	1.40	0.79

Note: Number of ions is based on 8 oxygens; total Fe is expressed as FeO*; na—not analyzed; Or—Orthoclase; Ab—Albite; An—Anorthite.

TABLE 5. REPRESENTATIVE ANALYSES OF MAJOR ELEMENTS FOR THE PYROXENES FROM THE METAMORPHIC SOLE ROCKS

	Gencek (Konya)							Şarkikaraağaç-Madenli (Isparta)								
Sample no.:	G15-4-1	G15-4-2	G15-4-3	G15-4-4	G15-4-6	G15-4-7	G15-4-8	S15-1-6	S15-1-5	S15-3-53	S15-3-52	S15-3-51	S15-3-66	S15-3-61	S15-3-85	S15-3-60
Major oxides (wt%)																
SiO_2	51.97	52.06	51.81	52.03	51.57	52.41	51.77	54.78	54.16	50.76	50.64	51.33	49.72	48.51	48.97	46.75
TiO_2	0.11	0.24	0.18	0.22	0.12	0.13	0.13	0.00	0.01	0.16	0.16	0.32	0.41	0.44	0.41	0.44
Al_2O_3	2.13	2.02	2.11	2.06	2.18	2.08	2.02	0.24	0.21	2.70	2.99	3.71	4.61	4.99	5.03	5.73
FeO*	10.30	9.74	11.01	9.69	10.72	10.06	10.63	3.63	4.61	10.94	11.58	11.12	10.69	11.63	11.53	13.86
MnO	0.33	0.15	0.30	0.45	0.16	0.31	0.28	0.18	0.21	0.20	0.40	0.14	0.23	0.06	0.21	0.51
MgO	11.72	12.28	11.83	12.32	11.65	12.19	11.78	16.82	16.11	11.31	10.40	10.79	11.35	10.21	10.24	8.62
CaO	22.35	22.81	22.00	22.60	21.71	22.29	21.94	25.84	25.44	22.71	21.84	20.65	22.20	22.12	22.39	20.98
Na_2O	1.14	1.01	1.07	0.83	1.07	1.16	1.22	0.11	0.23	1.25	1.54	2.10	1.28	1.26	1.21	1.81
K_2O	0.00	0.01	0.04	0.01	0.01	0.00	0.00	0.00	0.00	0.00	0.00	0.02	0.01	-0.01	0.01	0.01
Total	100.06	100.31	100.36	100.22	99.18	100.64	99.78	101.61	100.97	100.03	99.55	100.18	100.51	99.20	100.00	98.70
Si	1.94	1.94	1.93	1.94	1.95	1.94	1.94	1.97	1.97	1.90	1.91	1.91	1.85	1.83	1.84	1.79
Ti	0.00	0.01	0.01	0.01	0.00	0.00	0.00	0.00	0.00	0.00	0.00	0.01	0.01	0.01	0.01	0.01
Al	0.09	0.09	0.09	0.09	0.10	0.09	0.09	0.01	0.01	0.12	0.13	0.16	0.20	0.22	0.22	0.26
Cr	0.00	0.00	0.00	0.00	0.00	0.00	0.00	0.00	0.00	0.00	0.00	0.00	0.00	0.00	0.00	0.00
Fe^{3+}	0.10	0.10	0.11	0.08	0.08	0.10	0.11	0.06	0.07	0.17	0.16	0.16	0.18	0.18	0.17	0.28
Fe^{2+}	0.22	0.20	0.23	0.22	0.25	0.21	0.22	0.05	0.07	0.17	0.21	0.19	0.15	0.19	0.19	0.16
Mn	0.01	0.00	0.01	0.01	0.01	0.01	0.01	0.01	0.01	0.01	0.01	0.00	0.01	0.00	0.01	0.02
Mg	0.65	0.68	0.66	0.68	0.65	0.67	0.66	0.90	0.87	0.63	0.58	0.60	0.63	0.57	0.57	0.49
Ca	0.89	0.91	0.88	0.90	0.88	0.88	0.88	1.00	0.99	0.91	0.88	0.82	0.88	0.90	0.90	0.86
Na	0.08	0.07	0.08	0.06	0.08	0.08	0.09	0.01	0.02	0.09	0.11	0.15	0.09	0.09	0.09	0.13
K	0.00	0.00	0.00	0.00	0.00	0.00	0.00	0.00	0.00	0.00	0.00	0.00	0.00	0.00	0.00	0.00
Total	4.00	4.00	4.00	4.00	4.00	4.00	4.00	4.00	4.00	4.00	4.00	4.00	4.00	4.00	4.00	4.00
En	0.37	0.38	0.37	0.38	0.37	0.38	0.37	0.46	0.45	0.37	0.35	0.37	0.38	0.35	0.34	0.32
Fs	0.12	0.11	0.13	0.12	0.14	0.12	0.12	0.03	0.03	0.10	0.13	0.12	0.09	0.11	0.12	0.11
Wo	0.51	0.51	0.50	0.50	0.49	0.50	0.50	0.51	0.51	0.53	0.53	0.51	0.53	0.54	0.54	0.57

Note: Number of ions is based on 6 oxygens; total Fe is expressed as FeO*. En—Enstatite; Fs—Ferrosilite; Wo—Wollastonite.

($Ab_{92–97}$), anorthoclase ($Or_{11–26}$; $Ab_{70–84}$), and orthoclase ($Or_{52–98}$) end members (Fig. 8C). In the Şarkikaraağaç-Madenli area, feldspars are also altered, and they have albite ($Ab_{97–98}$), oligoclase ($Ab_{72–88}$), anorthoclase ($Or_{12–23}$; $Ab_{73–87}$), and orthoclase ($Or_{35–75}$) end members (Fig. 8C). A sample from the Madenli area metamorphic sole (S15-1) had very highly calcic plagioclases ($An_{92–93}$; Fig. 8C). The high-An plagioclases are associated with zeolites (thomsonite) that formed during hydrothermal alteration. Orthoclases are preserved in veins cutting the amphibole-rich phases, suggesting that hydrothermal alteration was strong in the oceanic environment (Vanko and Laverne, 1998).

PRESSURE AND TEMPERATURE CONDITIONS

Temperature conditions at the time of metamorphism for the metamorphic sole rocks in the Şarkikaraağaç-Madenli (Isparta) and Gencek (Konya) regions were calculated using the hornblende-plagioclase thermometer of Holland and Blundy (1994). This thermometer performs well (±40 °C) in the range 400–1000 °C and 1–15 kbar (Holland and Blundy, 1994). As quartz is absent in the assemblage, the edenite-richterite thermometer was used in the formula. The thermometer was applied to several amphibole and plagioclase pairs in contact with each other. In the Gencek region, sample G14-1 yielded temperatures ranging from 530 °C to 610 °C. In the Şarkikaraağaç-Madenli region, a temperature range was calculated from 480 °C to 520 °C for sample S14-1, from 550 °C to 700 °C for sample S14-4, and from 575 °C to 600 °C for sample S15-3. A strong correlation between increasing Al contents of amphiboles and increasing pressure makes it possible to use an Al-in-amphibole barometer (Hammarstrom and Zen, 1986; Hollister et al., 1987; Johnson and Rutherford, 1989; Schmidt, 1992). Applying this geobarometer for the amphibolites in the Şarkikaraağaç-Madenli region, samples S14-1, S14-4, and S15-3 yielded a pressure range from 5.4 to 7.9 kbar. In comparison, Gencek region samples G14-1, G14-4, G15-3, and G15-4 yielded a pressure range from 4.7 to 6.7 kbar. As a result, pressure-temperature (*P-T*) conditions of ~5.7 ± 1.0 kbar and 570 ± 40 °C were calculated for the metamorphism of amphibolites from the Gencek region, and *P-T* conditions of ~6.65 ± 1.3 kbar and 590 ± 110 °C were calculated for the metamorphism of amphibolites from the Şarkikaraağaç-Madenli region. The metamorphic pressures estimated for the amphibolite-facies rocks suggest metamorphism at depths of 17–20 km. *P-T* estimates for the amphibolites of the metamorphic sole in the study area are in accordance with *P-T* conditions of metamorphic sole rocks from other Tauride ophiolites (Çelik and Delaloye, 2003, 2006; Çelik, 2007), except the ones with blueschist overprints in the Bolkardağ area (Central Taurides) at 8–12 kbar and >560 °C (Dilek and Whitney, 1997) and those in the Tavşanlı area (northwest Turkey) at ~12 kbar and 425 °C (Okay et al., 1998; Plunder et al., 2016).

GEOCHEMISTRY

Bulk-rock major- and trace-element concentrations of the amphibolites and the isolated dikes are presented in Tables 1 and 2. The loss on ignition (LOI) values range from 1.19% to 7.96% for the amphibolites and from 2.04% to 4.63% for the isolated dikes, reflecting variable alteration, which is also indicated by the presence of secondary mineral phases (i.e., epidote, calcite, and chlorite) as described in the

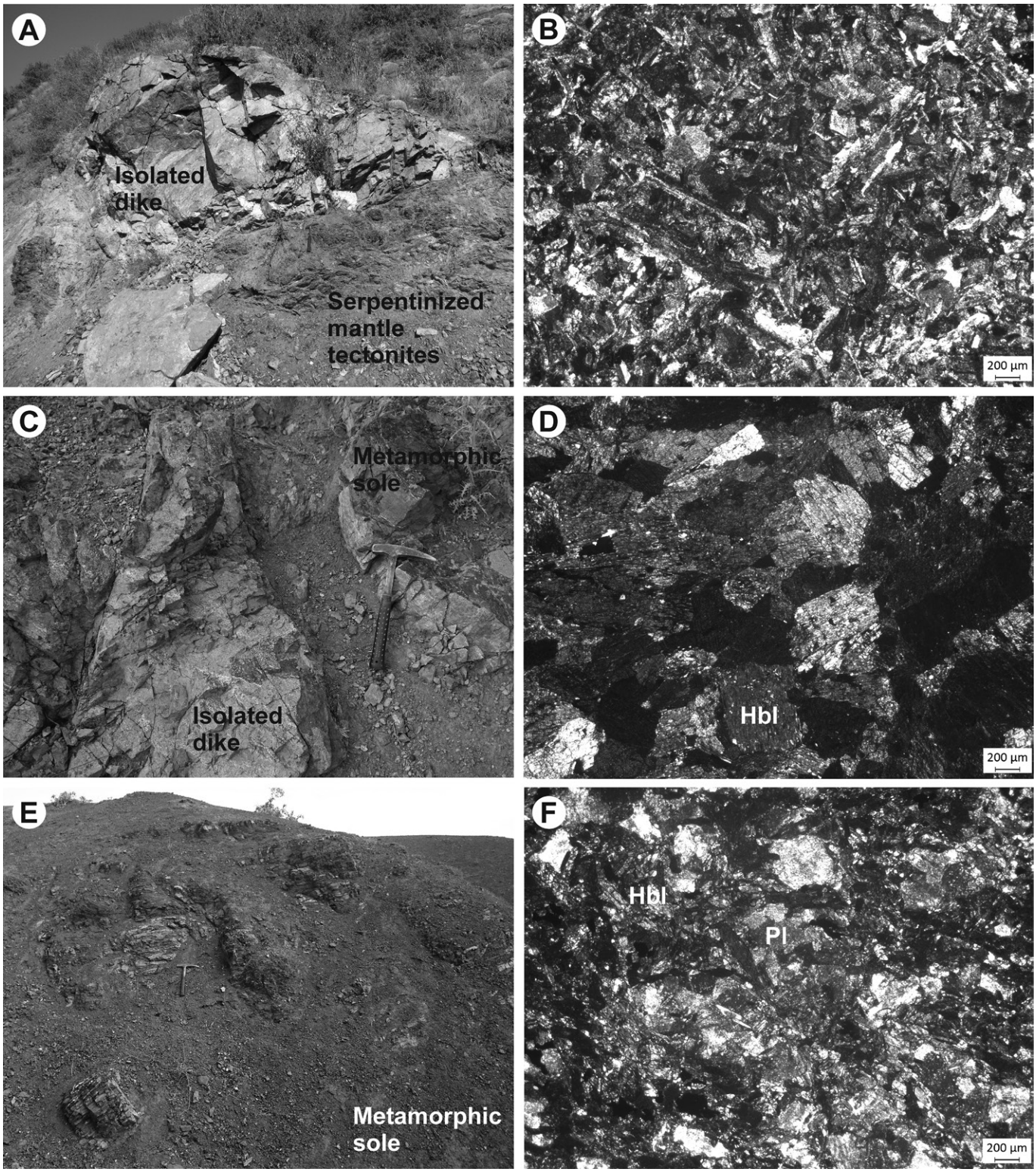

Figure 7. (A) Field view of the isolated dike cutting the serpentinized mantle tectonites. (B) Photomicrograph of the isolated dike. (C) Isolated dike cutting the metamorphic sole. (D) Photomicrograph of the amphibolite. (E) Field view of the foliated amphibolite. (F) Photomicrograph of the plagioclase amphibolite. Hbl—hornblende; Pl—plagioclase. Rock hammer for scale in A, C, and E.

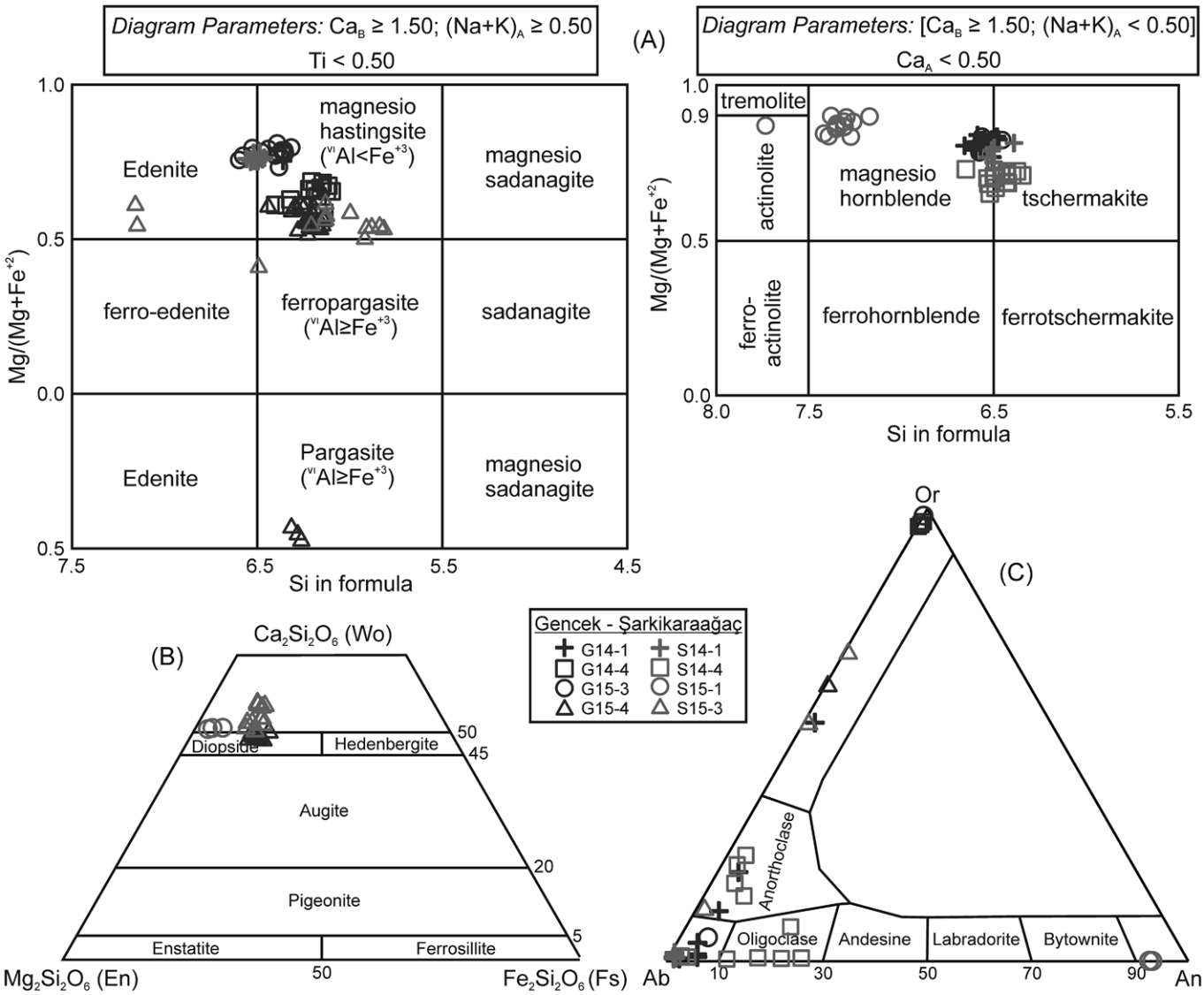

Figure 8. (A) Chemical composition of amphiboles in amphibolites from the Beyşehir-Hoyran Nappes (classification after Leake et al., 1997). (B) Chemical composition of pyroxenes in amphibolites (classification after Morimoto, 1988). (C) Feldspar compositions in the amphibolites. Or—orthoclase; Ab—Albite; An—Anorthite.

petrography section. Mobility of major and trace elements (large ion lithophile elements [LILEs]) is observed due to alteration after formation of a rock (Hart et al., 1974; Humphris and Thompson, 1978; Thompson, 1991). Petrological characterization of the studied rocks is based on rare earth elements (REEs) and high field strength elements (HFSEs), which are resistant to alteration (Floyd and Winchester, 1978; Pearce and Cann, 1973).

The isolated dikes from the north (Şarkikaraağaç and Madenli) and south (Gencek) of Lake Beyşehir display two distinct geochemical characters based on their Nb/Y ratio (0.03–1.72). The isolated dikes cutting the mantle tectonites in Şarkikaraağaç (S14-2) and Gencek areas are represented by tholeiitic basalts, whereas the isolated dike (S15-2) cutting the metamorphic sole in the Madenli area is characterized by alkali basalts (Fig. 9A). The amphibolitic metamorphic sole rocks from the north (Madenli) and south (Gencek) of Lake Beyşehir are exclusively represented by alkaline basaltic rock types based on their Nb/Y (0.96–2.25) and Zr/Ti (0.010–0.016) ratios (Fig. 9A; Pearce, 1996).

Various ratio/ratio plots of incompatible elements were used in Figures 9B and 9C to characterize mantle source affinities for the isolated dikes and the protoliths of the metamorphic sole rocks from the Beyşehir-Hoyran ophiolite. Comparative trace-element ratios for different geochemical groups of the studied rocks were plotted together with those of mid-ocean-ridge basalt (MORB) and ocean-island basalt (OIB). The Y/Nb, Y/Ta, Zr/Nb, and Ti/Nb ratios of the isolated dikes from the Şarkikaraağaç-Madenli areas display geochemical characters similar to both normal mid-ocean-ridge basalt (N-MORB) and OIB (Figs. 9B and 9C). The isolated dikes in the Gencek area are more akin to N-MORB (Figs. 9B and 9C). The Y/Nb, Y/Ta, Zr/Nb, and Ti/Nb ratios of the metamorphic sole rocks from the Madenli and Gencek areas are identical to OIBs (Figs. 9B and 9C).

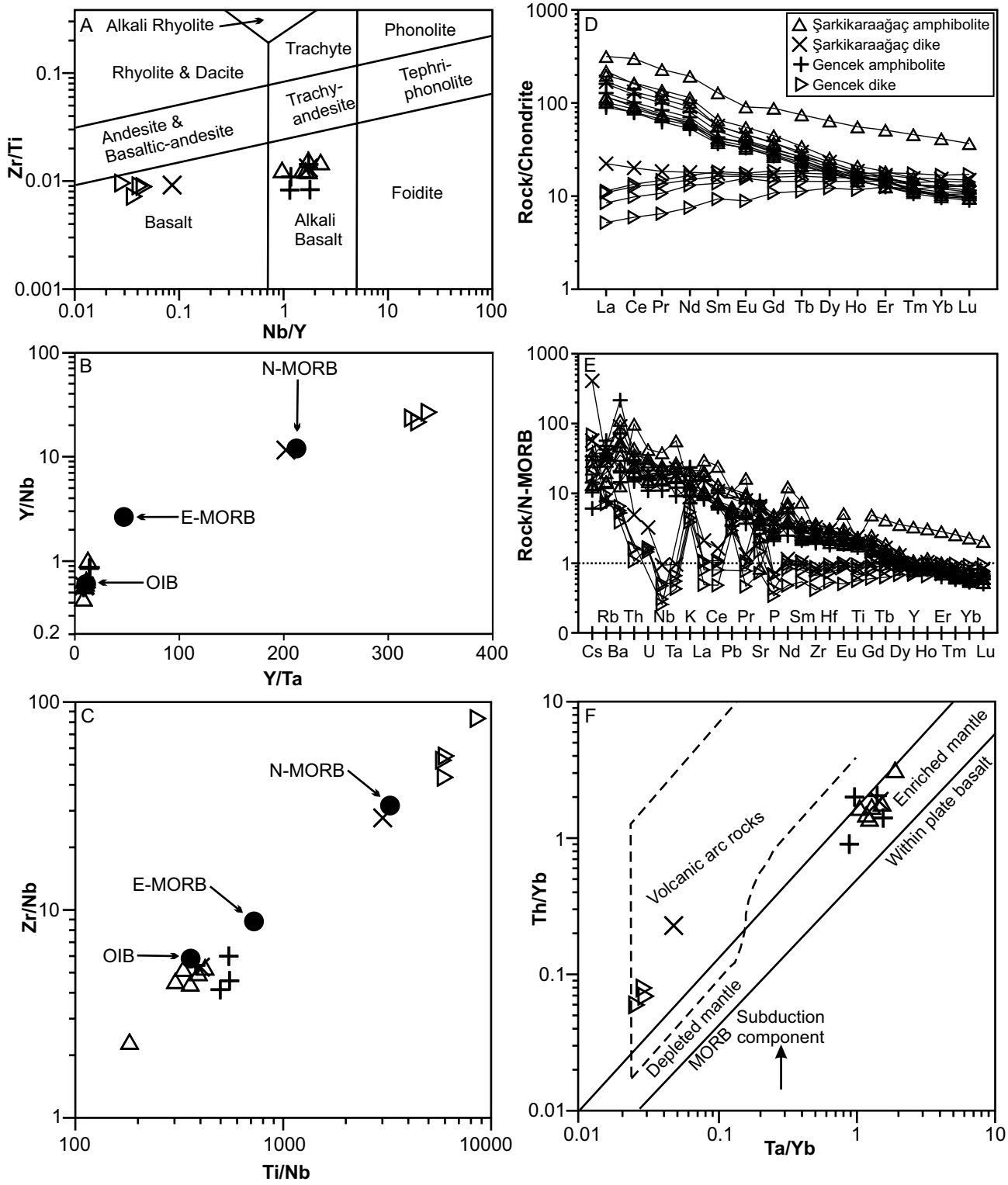

Figure 9. (A) Zr/Ti vs. Nb/Y diagram (after Pearce, 1996) for the isolated dikes and the amphibolites. (B) Y/Nb vs. Y/Ta and (C) Zr/Nb vs. Ti/Nb diagrams, indicating different magma sources for the protoliths of the metamorphic sole rocks and isolated dikes. N-MORB—normal mid-ocean-ridge basalt; E-MORB—enriched MORB; OIB—oceanic-island basalt. (D) Chondrite-normalized rare earth element (REE) and (E) N-MORB normalized multi-element diagrams for the metamorphic sole rocks and the isolated dikes (normalizing values are from Sun and McDonough, 1989). (F) Th/Yb vs. Ta/Yb diagram (after Pearce, 1982) for the metamorphic sole rocks and isolated dikes in the Beyşehir-Hoyran Nappes.

A chondrite-normalized REE diagram for the isolated diabase dikes and the metamorphic sole rocks is given in Figure 9D. The tholeiitic isolated dikes cutting the mantle tectonites from the north (Şarkikaraağaç) and south (Gencek) of Lake Beyşehir have flat to slightly LREE-depleted character (La/Yb_N = 1.46–0.41) and overall REE abundances between 5× and 22× chondritic (Fig. 9D). The alkaline isolated dike cutting the metamorphic sole in the Madenli area (north of Lake Beyşehir) exhibits enrichment in light rare earth elements (LREEs; La_N/Yb_N = 14.06) with overall REE abundances between 11× and 169× chondritic (Fig. 9D). The alkaline metamorphic sole amphibolites from the Şarkikaraağaç (north) and Gencek (south) regions display similar REE patterns, characterized by LREE enrichments (La_N/Yb_N = 7.6–22.3) with overall REE abundances ranging from 9× to 315× chondritic values (Fig. 9D). A N-MORB–normalized multi-element diagram for the isolated dikes and the metamorphic sole rocks is given in Figure 9E. The tholeiitic isolated dikes cutting the mantle tectonites from the north (Şarkikaraağaç) and south (Gencek) of Lake Beyşehir exhibit similar enrichment/depletion patterns relative to N-MORB (Fig. 9E), including: (1) LILE variations (Cs, Rb, Ba, K, Pb, etc.), (2) strong negative Nb (Ta) anomalies, and (3) flat-lying HFSE patterns. The elevated concentrations of LILEs relative to HFSEs in subduction zone magmas most likely originate from fluids and/or siliceous melts derived from the subducting oceanic slab. These slab-derived fluids carry high concentrations of LILEs, while the HFSEs, most notably Nb, are retained in the slab (Arculus and Powel, 1986; Pearce, 1982; Wallin and Metcalf, 1998; Yogodzinski et al., 1994). Therefore the negative Nb (Ta) anomaly is clearly intrinsic to the parental magma of the isolated dikes. Th enrichment relative to other incompatible elements is interpreted as an indication of a subduction zone component (Pearce, 1983; Wood et al., 1979). The negative Nb (Ta) and positive Th anomalies suggest a suprasubduction zone setting for their genesis. The alkaline isolated dikes cutting the metamorphic sole in the Şarkikaraağaç-Madenli (north) area display strong progressive enrichment (HFSE to LILE) patterns and have more in common with typical enriched OIB composition (Sun and McDonough, 1989). MORB-normalized trace-element patterns of alkaline amphibolites also display progressive enrichment (HFSE to LILE) patterns, comparable with within-plate basalt and OIB settings (Pearce, 1982). The alkaline amphibolites from the metamorphic sole beneath the eastern Mediterranean ophiolites are a very conspicuous feature of a particular magma source affinity (Çelik, 2007; Çelik and Delaloye, 2003, 2006; Elitok and Drüppel, 2008; Lytwyn and Casey, 1995; Parlak et al., 1995a, 2006; Polat et al., 1996; Vergili and Parlak, 2005).

Pearce (1982) documented that a Th/Yb versus Ta/Yb ratio-ratio plot can be used to discriminate between depleted mantle (MORB) and enriched mantle (intraplate) sources, based on the fact that the addition of slab-derived fluids/melts results in an increase in Th/Yb in the mantle source (Fig. 9F). The tholeiitic isolated dikes cutting the mantle tectonites in Gencek (south) and in Şarkikaraağaç (north) plot near the depleted mantle source region, but they show elevated Th/Yb ratioa, indicating involvement of subduction zone fluids. In contrast, the alkaline amphibolites from both regions and the alkaline isolated dike cutting the metamorphic sole (amphibolites) in the Madenli area plot within the enriched mantle source/intraplate basalt region without any subduction zone influence (Fig. 9F).

GEOCHRONOLOGY

U-Pb Dating

Eighteen mineral phases (zircon and titanite) out of 11 samples from the metamorphic sole amphibolites and the isolated dikes cutting the mantle tectonites of the ophiolitic rocks from the Beyşehir-Hoyran Nappes in the Central Taurides were used for LA-SF-ICP-MS U-Pb dating.

Şarkikaraağaç (Isparta) Region

One isolated dike cutting the mantle tectonite and three amphibolites from the metamorphic sole were used for U-Pb dating in this region. Sample S14-2 was collected from an isolated dike. Six zircons from the sample form 20–50 μm, stubby, colorless, and translucent crystals (Supplementary File 1 [see footnote 1]). The CL images show that zircon crystals are unzoned, and their Th/U ratios range from 0.02 to 0.27. Six zircons yielded a 87.6 ± 2.1 Ma lower-intercept age (Fig. 10). Eleven titanite crystals were analyzed from the same sample (S14-2), and they yielded an 88.6 ± 6.1 Ma lower-intercept age (Fig. 10).

Sample S14-3 was collected from an amphibolite. Nine zircons from the sample form 20–60 μm, prismatic, rounded-stubby, subhedral, colorless, and semitranslucent crystals. The CL images of the crystals show patchy zoning, cloudy zoning, and oscillatory zoning overprinted by homogeneous recrystallized domains consistent with growth in the solid state (Hoskin and Black, 2000; see also Supplementary File 2 [footnote 1 herein]). Th/U ratios range from 0.05 to 0.26. Seven out of nine zircons yielded a 91.1 ± 2.1 Ma lower-intercept age (Fig. 10). Fifteen titanite crystals from the same sample (S14-3) were analyzed and yielded a 92.5 ± 4.9 Ma lower-intercept age (Fig. 10). Sample S14-4 was collected from an amphibolite. Thirty-one zircons from the sample form 20–60 μm, subhedral, prismatic with slightly rounded tips and edges, colorless, and translucent crystals (Supplementary File 2). The CL images of the crystals show patchy zoning and sector zoning overprinted by a recrystallized domain consistent with growth in the solid state (Hoskin and Black, 2000). Th/U ratios range from 0.01 to 0.95. Twenty-three out of 31 zircons yielded an 89.8 ± 1.2 Ma lower-intercept age (Fig. 10). Twenty-one titanite crystals from the same sample (S14-4) were analyzed and yielded a 90.0 ± 9.4 Ma lower-intercept age (Fig. 10). Sample S14-5 was collected from an amphibolite. Thirty-five zircons from the sample form 30–90 μm, stubby, prismatic, colorless, and semitranslucent crystals (Supplementary File 2). The CL images of the crystals show slightly patchy zoning and sector zoning. Th/U ratios range from 0.03 to 0.69. Ten out of 35 zircons yielded a concordia age of 88.85 ± 0.98 Ma (Fig. 10). Fifteen titanite crystals from the same sample (S14-5) were analyzed and yielded a 92.9 ± 5.9 Ma lower-intercept age (Fig. 10).

Madenli (Isparta) Region

One amphibolite from the metamorphic sole was used for U-Pb dating in this region. Sample S14-1 was collected from an amphibolite. Thirteen titanite crystals from the sample were analyzed, and they yielded a 91.2 ± 3.9 Ma lower-intercept age (Fig. 11).

Gencek (Konya) Region

Three isolated dikes cutting the mantle tectonites and three amphibolites from the metamorphic sole were used for U-Pb dating in this region. Sample G14-2 was collected from an isolated dike. Seven titanite crystals were analyzed, and they yielded a 102.3 ± 7.4 Ma lower-intercept age (Fig. 11). Sample G14-3 was collected from an isolated dike. Fifteen titanite crystals were analyzed, and they yielded a 94.9 ± 5.6 Ma lower-intercept age (Fig. 11). Sample G14-5 was collected from an isolated dike. Six zircons from the sample form 20–50 μm, stubby, subhedral, colorless, and translucent crystals (Supplementary File 1). The CL images show that zircon crystals have weak sector zoning, and their Th/U ratios range from 0.05 to 0.28. Six zircons yielded a 90.8 ± 1.6 Ma lower-intercept age (Fig. 11). Seven titanite crystals

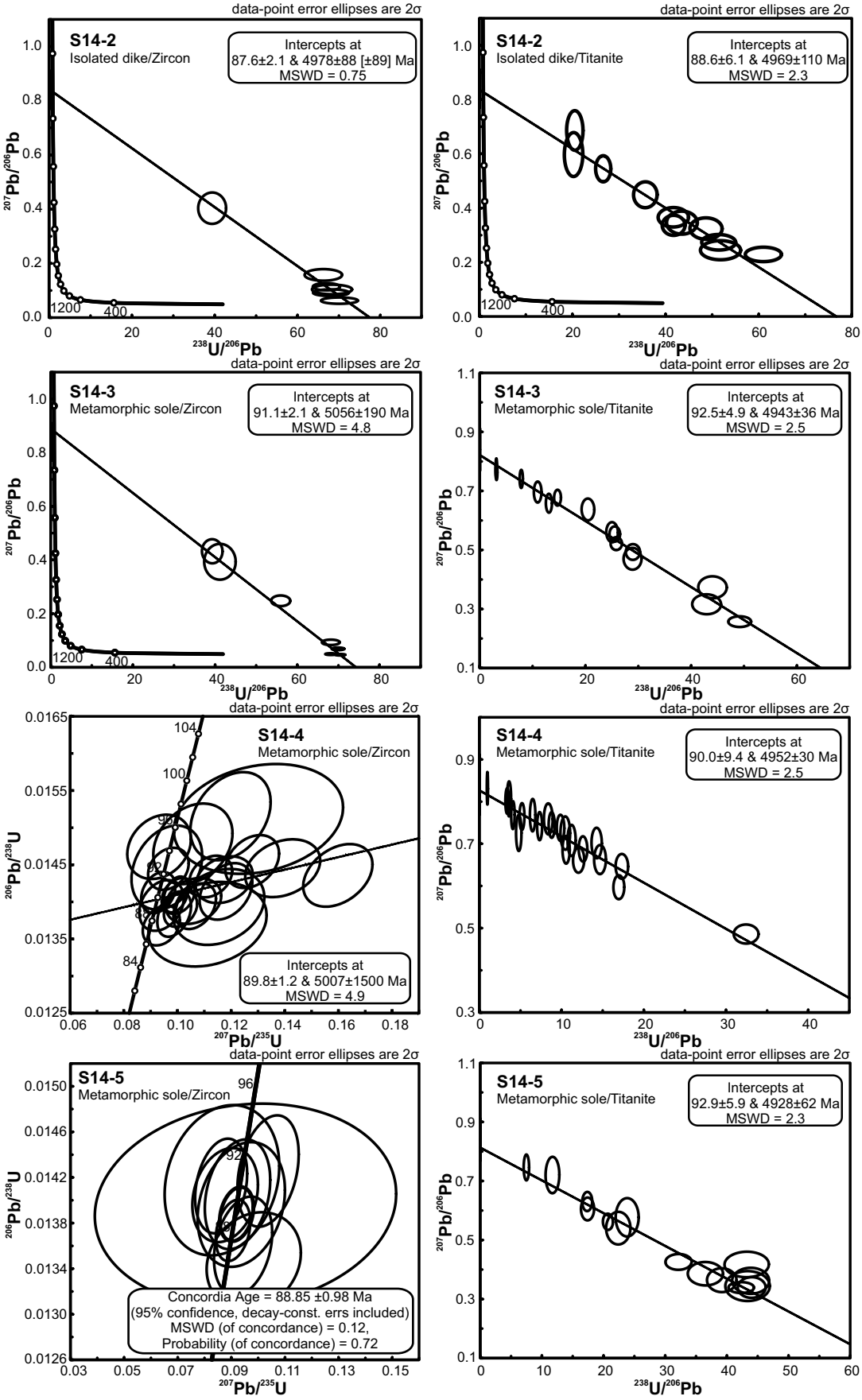

Figure 10. Zircon and titanite U-Pb ages for the isolated dikes and metamorphic sole amphibolites in the Şarkikaraağaç (Isparta) region. MSWD—mean square of weighted deviates.

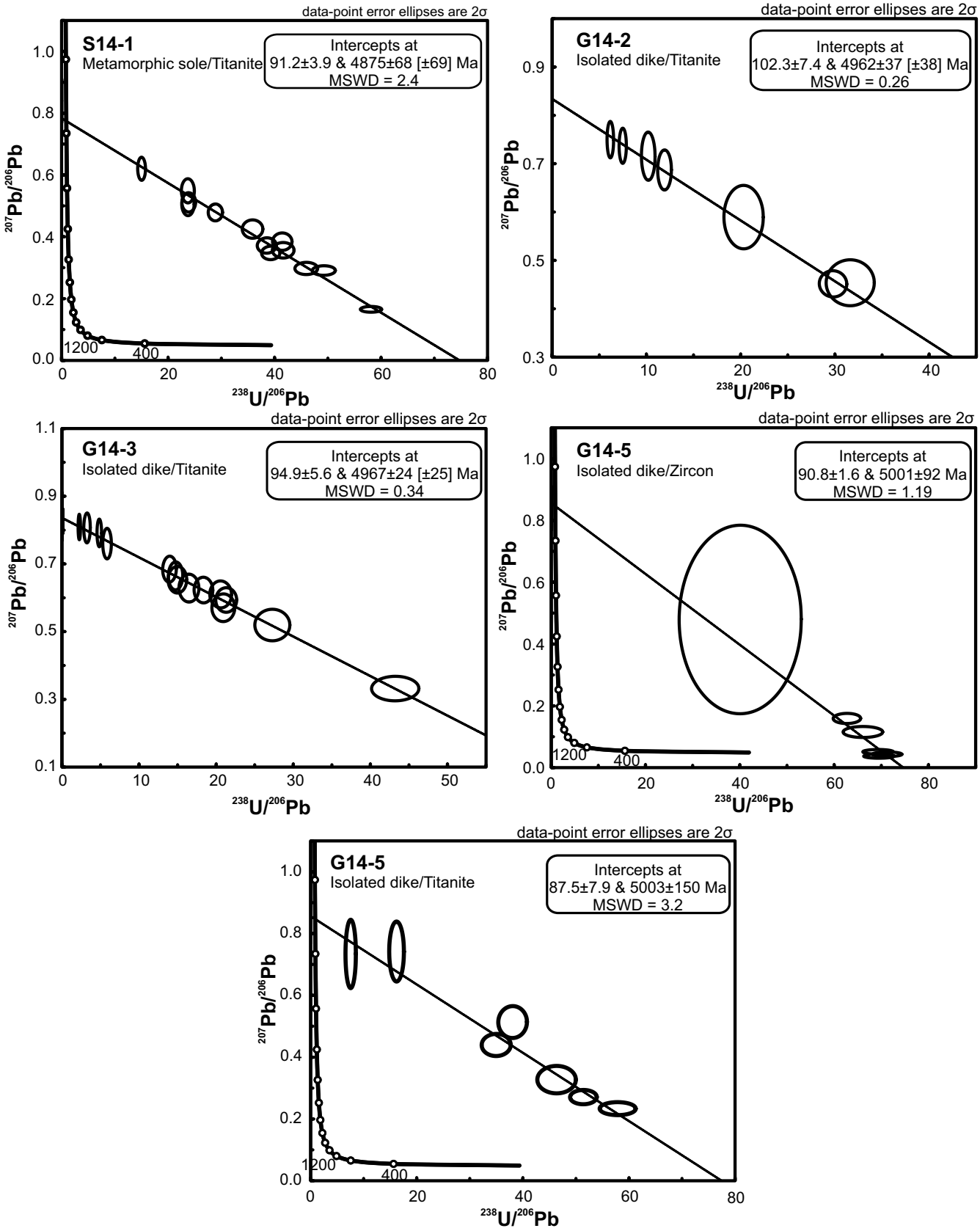

Figure 11. Zircon and titanite U-Pb ages for the metamorphic sole rocks in the Madenli (Isparta) area and isolated dikes in the Gencek (Konya) area. MSWD—mean square of weighted deviates.

from the same sample (G14-5) were analyzed, and they yielded a 87.5 ± 7.9 Ma lower-intercept age (Fig. 11).

Sample G14-1 was collected from an amphibolite. Eighteen zircons from the sample form 10–40 μm, stubby, subhedral, colorless, and semitranslucent crystals (Supplementary File 3 [see footnote 1]). The CL images show that zircon crystals have either weak oscillatory zoning or cloudy zoning, and their Th/U ratios range from 0.16 to 0.51. Twelve out of 18 zircons yielded a concordia age of 89.74 ± 0.87 Ma (Fig. 12). Fifteen titanite crystals from the same sample (G14-1) were analyzed, and they yielded a 92.8 ± 6.0 Ma lower-intercept age (Fig. 12). Sample G15-4 was collected from an amphibolite. Eighteen zircons form 30–50 μm, stubby, subhedral, colorless, and semitranslucent crystals (Supplementary File 3). The CL images show that zircon crystals have unzoned, cloudy, patchy, sector zoning, and their Th/U ratios range from 0.26 to 0.58. Eighteen zircons yielded a concordia age of 90.81 ± 0.73 Ma (Fig. 12). Twelve titanite crystals from the same sample (G15-4) were analyzed, and 10 out of 12 crystals yielded a 91.0 ± 6.0 Ma lower-intercept age (Fig. 12). Sample G15-3 was collected from an amphibolite. Fifteen titanite crystals from the sample were analyzed, and they yielded a 94.0 ± 4.8 Ma lower-intercept age (Fig. 12).

^{40}Ar-^{39}Ar Dating

Four new ^{40}Ar/^{39}Ar ages were obtained from amphibolites of the metamorphic soles to the north (Madenli: S14-1 and Şarkikaraağaç: S14-4) and the south (Gencek: G14-1 and G14-4) of Lake Beyşehir along the Beyşehir-Hoyran Nappes. All amphiboles analyzed were metamorphic in origin. The amphiboles in sample S14-1 are characterized as magnesiohastingsite, magnesiohornblende, edenite, and tschermakite (Fig. 8A). The amphiboles in sample S14-4 are characterized as tschermakite and magnesiohornblende (Fig. 8A). The amphiboles in sample G14-1 are represented by magnesiohornblende to tschermakite (Fig. 8A). The amphiboles in sample G14-4 are represented exclusively by magnesiohastingsite (Fig. 8A). Except sample G14-4, three of the amphiboles from the metamorphic sole rocks yielded robust ^{40}Ar/^{39}Ar plateau ages (Fig. 13).

Sample S14-1 yielded a plateau, including 16 of 24 steps with 95.7% of the total ^{39}Ar released, which gave weighted mean age of 91.40 ± 0.37 Ma (1σ; Fig. 13). Sample S14-4 yielded a plateau, including 13 of 19 steps with 79.5% of the total ^{39}Ar released, which gave a weighted mean age of 91.52 ± 0.43 Ma (1σ; Fig. 13). Sample G14-1 yielded an undisturbed age spectrum, in which all 15 steps with 100% of the released ^{39}Ar defined a plateau age of 93.71 ± 0.34 Ma (1σ; Fig. 13). Sample G14-4 yielded a discordant spectrum (Fig. 13). Discordant spectra for the sample are characterized by ages of ca. 40–80 Ma for increments comprising the first 10% of ^{39}Ar released. Discordance within the amphibole spectra could be due to a number of causes, including episodic loss or slow cooling, presence of separates and younger phases that degassed early, or recoil effects. One interpretation consistent with all of the ^{40}Ar/^{39}Ar analytical data is that the sample recorded the effects of overprinting low-grade metamorphic conditions that followed the high-grade Cretaceous crystallization event. A minimum estimate for the timing of crystallization or cooling to retention temperature is ca. 92 Ma, with subsequent ^{40}Ar* loss ending by ca. 48 Ma (mid-Eocene). The Ar-closure temperature in amphibole is assumed to be 510 ± 25 °C based on the diffusion experiments of Harrison (1982). Except sample G14-4, all age spectra of the amphiboles show generally flat release patterns, suggesting no thermal disturbance after cooling below 550 °C.

DISCUSSION

The Beyşehir-Hoyran Nappes in the Central Taurides originated from the Inner Tauride Ocean, which was bounded by the Tauride-Anatolide platform to the south and the Central Anatolian Crystalline Complex to the north. The two-phase Late Cretaceous and mid-Eocene southward emplacement of Tauride thrust sheets in the Beyşehir-Hoyran Nappes is well documented (Mackintosh and Robertson, 2013). After the first emplacement of the ophiolitic rocks southward onto the Tauride-Anatolide platform in Late Cretaceous time (Mackintosh and Robertson, 2013; Robertson and Dixon, 1984; Robertson et al., 2009; Şengör and Yılmaz, 1981), the ensuing continent-continent collision and rethrusting in the mid-Eocene placed the northerly derived carbonate platform units above the ophiolitic rocks and mélange that had been initially emplaced during latest Cretaceous time (Andrew and Robertson, 2002; Mackintosh and Robertson, 2013). The Mersin ophiolite and associated units exhibit many similarities to the Beyşehir-Hoyran Nappes, suggesting that they formed in the Inner Tauride Ocean and were emplaced to the north of the Tauride carbonate platform (Parlak and Robertson, 2004).

Interpretation of the Geochemical Data

Petrological and geochemical analyses indicate that the amphibolites are metamorphosed OIBs that are chemically different than the overlying ophiolitic crustal rocks. Çelik and Delaloye (2006) also reported alkaline amphibolites within the metamorphic sole from the Gencek (Konya) area. Similarly, Elitok and Drüppel (2008) documented alkaline to tholeiitic amphibolites from the Şarkikaraağaç-Madenli (Isparta) area, suggesting an origin derived from within-plate alkali basalt and tholeiitic island-arc basalts. Triassic–Jurassic alkaline seamount-type basalts have been commonly reported from Neotethyan sutures in Anatolia, namely, the İzmir-Ankara-Erzincan (Göncüoğlu et al., 2000, 2006, 2010; Parlak et al., 2013b; Rojay et al., 2001), the Bitlis-Zagros (Maury et al., 2008; Robertson and Waldron, 1990; Robertson et al., 2016; Varol et al., 2011), the Inner Tauride (Elitok and Drüppel, 2008; Parlak et al., 1995b; Polat et al., 1996; Robertson et al., 2009), and the Haybi volcanic rocks in Oman (Searle and Malpas, 1980).

The geochemistry of the isolated dikes cutting the mantle tectonites and the metamorphic soles in the region suggests two distinct magma sources. The tholeiitic dikes are compositionally similar to island-arc tholeiites (Gill, 1981). Modern analogues of the Late Cretaceous suprasubduction zone–type crustal rocks of ophiolites in Turkey are documented in forearc areas of the SW Pacific region (Bloomer and Hawkins, 1983; Pearce et al., 1992; Stern and Bloomer, 1992; Taylor, 1992), the Tonga arc, and Cape Vogel in Papua New Guinea (Kamenetsky et al., 2002). Flat to slightly LREE-depleted patterns and a strong Nb depletion in MORB-normalized multi-element diagrams for the studied tholeiitic isolated dikes display close similarity to crustal rocks in suprasubduction zone–type ophiolites from the Eastern Mediterranean region (Alabaster et al., 1982; Al-Riyami et al., 2002; Bağcı and Parlak, 2009; Bağcı et al., 2008; Beccaluva et al., 2004, 2005; Çelik and Chiaradia, 2008; Çelik and Delaloye, 2003; Dilek and Thy, 2009; Kavak et al., 2017; Parlak, 1996, 2000; Parlak et al., 2000, 2004, 2009, 2013b; Pearce, 2003; Pe-Piper et al., 2004; Saccani and Photiades, 2005; Rızaoğlu et al., 2006; Su et al., 2018; Vergili and Parlak, 2005; Yalınız et al., 1996, 2000). On the other hand, crustal rocks with enriched composition (dikes/gabbro) have also been reported from the Pozantı-Karsantı (Aladağ) ophiolite (Çelik, 2007), the Divriği (Sivas) ophiolite (Parlak et al., 2006), and the Tekirova (Antalya) ophiolite (Bağcı and Parlak, 2009). In Tauride ophiolites, isolated dike intrusions with island-arc tholeiitic to boninitic affinities are common, suggesting progressive source depletion. However, the isolated dike with alkaline composition cutting the metamorphic sole suggests that it was probably derived from an enriched mantle source within local fractures or tears in

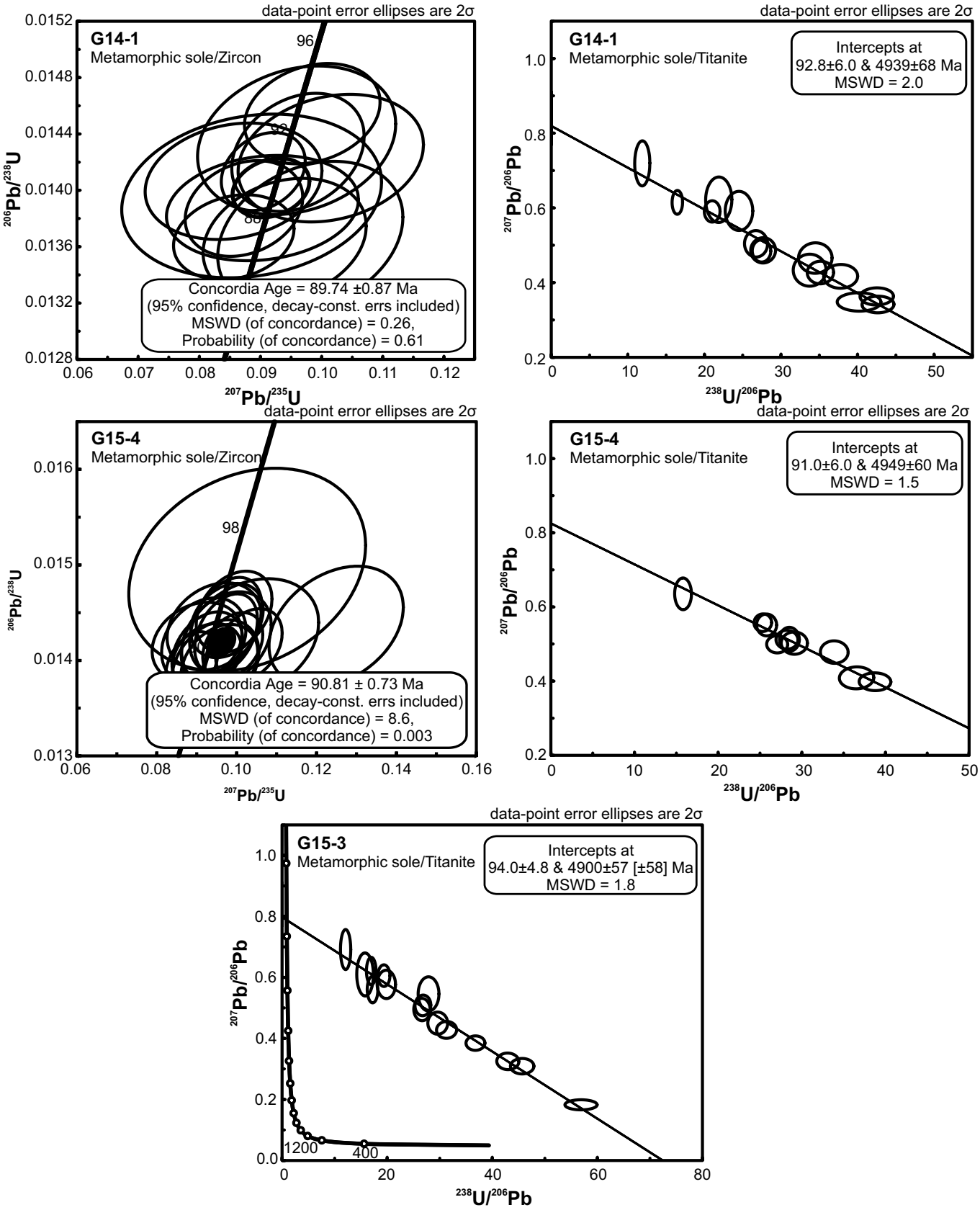

Figure 12. Zircon and titanite U-Pb ages for the metamorphic sole rocks in Gencek (Konya) area. MSWD—mean square of weighted deviates.

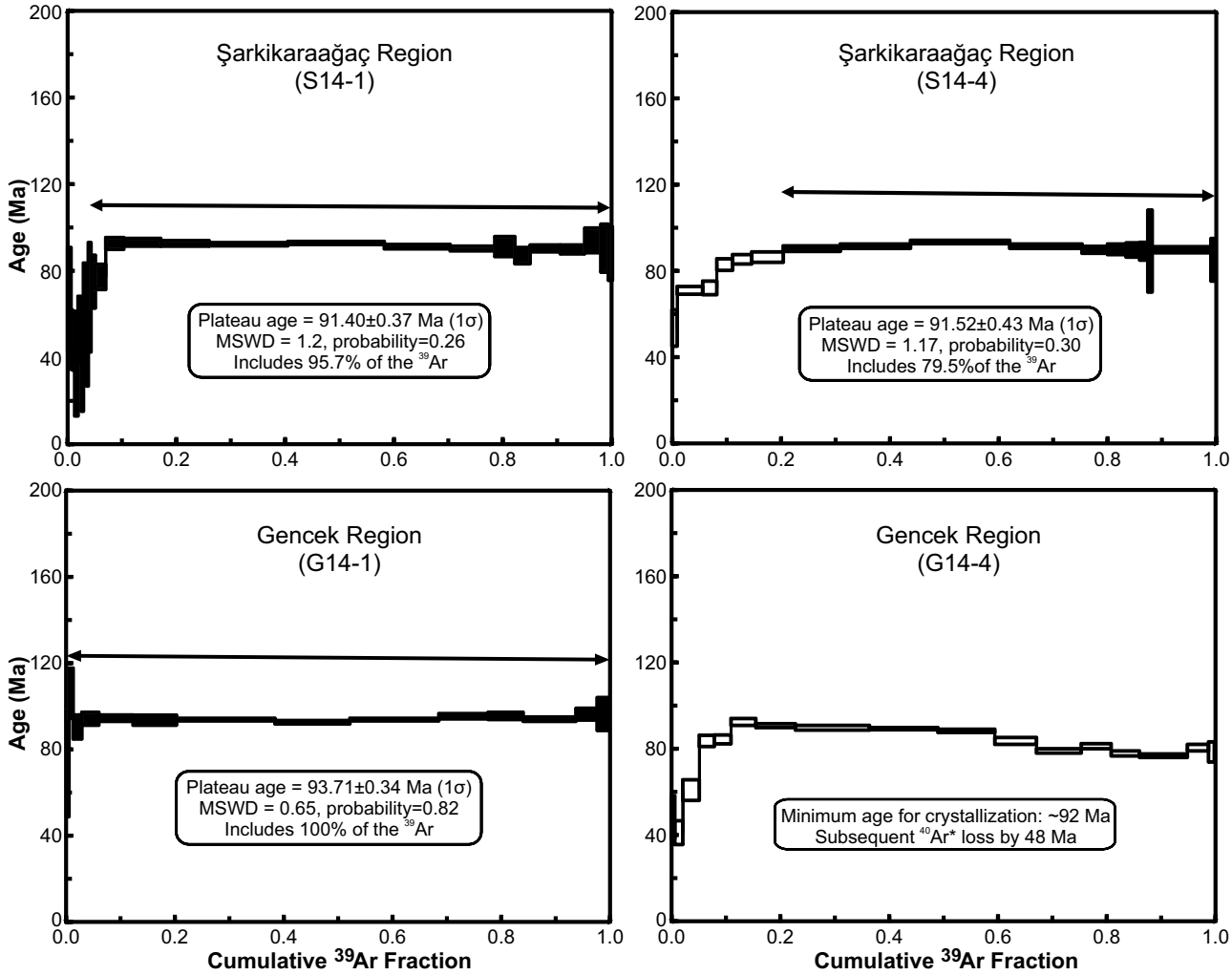

Figure 13. Amphibole ^{40}Ar-^{39}Ar age spectra from the metamorphic sole rocks in Şarkikaraağaç-Madenli (Isparta) and Gencek (Konya) regions. MSWD—mean square of weighted deviates.

the subducting plate. Such alkaline magmatism has been documented from crustal rocks of the Pozantı-Karsantı (Aladağ; Çelik, 2007), the Divriği (Sivas; Parlak et al., 2006), and the Tekirova (Antalya) ophiolites (Bağcı and Parlak, 2009).

Interpretation of the Geochronological Data

A summary of the tectonic setting of the dated metamorphic sole rocks and isolated dikes as well as the results of the U-Pb and ^{40}Ar-^{39}Ar ages for different mineral phases from the Şarkikaraağaç-Madenli (Isparta) and Gencek (Konya) regions in the Beyşehir-Hoyran Nappes is presented in Table 6. Zircon and titanite phases from the isolated dike sample (S14-2) in the Şarkikaraağaç (Isparta) area yielded 87.6 ± 2.1 Ma and 88.6 ± 6.1 Ma U-Pb isotopic ages. Moreover, zircon and titanite phases from the isolated dike sample (G14-5) in the Gencek (Konya) area yielded 90.8 ± 1.6 Ma and 87.5 ± 7.9 Ma U-Pb isotopic ages. The obtained ages are very similar to each other within analytical uncertainty (1σ). Radiogenic Pb* closure temperature was constrained as ~850–900 °C for zircon (Cherniak and Watson, 2001) and 550–650 °C for titanite (Cherniak, 1993). The identical U-Pb ages of different mineral phases with different closure temperatures for the isolated dikes in both regions suggest that oceanic crust cooled very rapidly (Fig. 14). In addition, two isolated dike samples in the Gencek (Konya) region yielded 102.3 ± 7.4 Ma (G14-2) and 94.9 ± 5.6 Ma (G14-3) titanite U-Pb ages (Table 6). In analytical uncertainty (1σ), these ages overlap with the ages of the aforementioned isolated dike samples (Fig. 14). Therefore, all the U-Pb ages from different mineral phases (zircon and titanite) should be interpreted as the crystallization age of magmatic growth of the oceanic crust.

In the Madenli (Isparta) region, titanite from the metamorphic sole sample (S14-1) yielded a 91.2 ± 3.9 Ma U-Pb age. Amphibole separates from the same sample (S14-1) yielded a 91.4 ± 0.4 Ma ^{40}Ar-^{39}Ar age (Table 6). In the

TABLE 6. SUMMARY OF U-Pb ZIRCON AND TITANITE AND ^{40}Ar-^{39}Ar AMPHIBOLE ISOTOPIC AGES FOR THE METAMORPHIC SOLE ROCKS AND ISOLATED DIKES IN THE BEYŞEHIR-HOYRAN NAPPES

Beyşehir-Hoyran Nappes (ophiolite) Sample no.:	Mineral phase	U-Pb concordia age (Ma ± 1σ)	U-Pb lower-intercept age (Ma ± 1σ)	$^{40}Ar/^{39}Ar$ plateau age (Ma ± 1σ)	Unit	Tectonic setting
Şarkikaraağaç (Isparta)						
S14-2	Zrn/Ttn		87.6 ± 2.1/88.6 ± 6.1		Isolated dike cutting mantle tectonite	IAT
S14-3	Zrn/Ttn		91.1 ± 2.1/92.5 ± 4.9		Met. sole	OIB
S14-4	Zrn/Ttn/Am		89.8 ± 1.2/90.0 ± 9.4	91.52 ± 0.43	Met. sole	OIB
S14-5	Zrn/Ttn	88.85 ± 0.98	92.9 ± 5.9		Met. sole	OIB
Madenli (Isparta)						
S14-1	Ttn/Am		91.2 ± 3.9	91.4 ± 0.37	Met. sole	OIB
Gencek (Konya)						
G14-1	Zrn/Ttn/Am	89.74 ± 0.87	92.8 ± 6.0	93.71 ± 0.34	Met. sole	OIB
G14-4	Am			Ca. 92, subsequent $^{40}Ar^*$ loss by ca. 48	Met. sole	OIB
G15-3	Ttn		94.0 ± 4.8		Met. sole	OIB
G15-4	Zrn/Ttn	90.81 ± 0.73	91.0 ± 6.0		Met. sole	OIB
G14-2	Ttn		102.3 ± 7.4		Isolated dike cutting mantle tectonite	IAT
G14-3	Ttn		94.9 ± 5.6		Isolated dike cutting mantle tectonite	IAT
G14-5	Zrn/Ttn		90.8 ± 1.6/87.5 ± 7.9		Isolated dike cutting mantle tectonite	IAT
B-192*	Am			90.9 ± 1.3	Met. sole	OIB
B-194*	Am			91.5 ± 1.9	Met. sole	OIB

Note: Zrn—zircon; Ttn—titanite; Am—amphibole; Met.—metamorphic; OIB—oceanic-island basalt; IAT—island-arc tholeiite.
*Samples B-192 and B-194 were taken from Çelik et al. (2006).

Şarkikaraağaç (Isparta) region, zircon and titanite from the metamorphic sole sample (S14-3) yielded 91.1 ± 2.1 Ma and 92.5 ± 4.9 Ma U-Pb ages (Table 6). Zircon and titanite phases from the metamorphic sole sample (S14-4) yielded 89.8 ± 1.2 Ma and 90.0 ± 9.4 Ma U-Pb ages. Amphibole separates from the same sample (S14-4) yielded a 91.52 ± 0.43 Ma ^{40}Ar-^{39}Ar age (Table 6). Zircon and titanite phases from the metamorphic sole sample (S14-5) yielded 88.85 ± 0.98 Ma and 92.9 ± 5.9 Ma U-Pb ages (Table 6). In the Gencek (Konya) region, zircon and titanite from the metamorphic sole sample (G14-1) yielded 89.74 ± 0.87 Ma and 92.8 ± 6.0 Ma U-Pb ages. Amphibole separates from the same sample (G14-1) yielded a 93.71 ± 0.34 Ma ^{40}Ar-^{39}Ar age (Table 6). Titanite from the metamorphic sole sample (G15-3) yielded a 94.0 ± 4.8 Ma U-Pb age (Table 6). Zircon and titanite phases from the metamorphic sole sample (G15-4) yielded 90.81 ± 0.73 Ma and 91.0 ± 6.0 Ma U-Pb ages. Amphibole separates from the metamorphic sole sample (G14-4) yielded a ca. 92 Ma minimum ^{40}Ar-^{39}Ar age (Table 6).

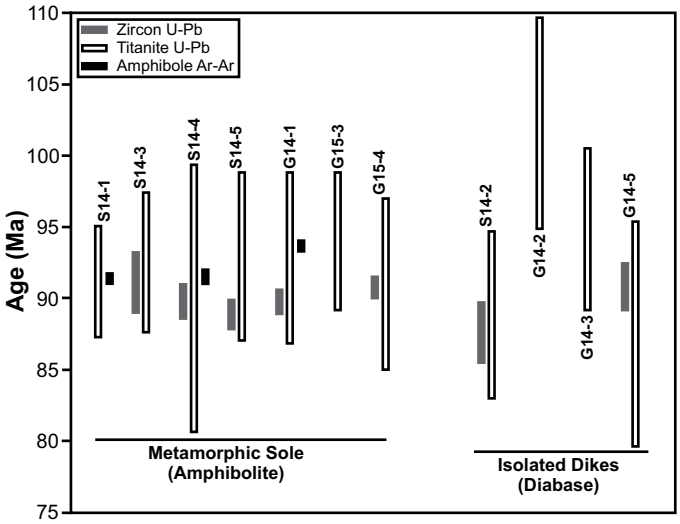

Figure 14. Compilation of zircon and titanite U-Pb and amphibole ^{40}Ar-^{39}Ar ages for the metamorphic sole rocks and isolated dikes in the Beyşehir-Hoyran ophiolite.

Metamorphic zircons may be produced by intragrain reworking of previously formed zircon under certain *P-T* conditions ($T \geq 400$ °C). These processes are defined as recrystallization (Corfu et al., 2003; Geisler et al., 2001; Hoskin and Black, 2000; Hoskin and Schaltegger, 2003; Pidgeon, 1992; Pidgeon et al., 1998; Rizvanova et al., 2000; Tomaschek et al., 2003; Wu and Zheng, 2004). During these processes, protolith zircons are partly or wholly reconstructed without any new zircon growth. Th/U ratios of the zircons in the metamorphic sole rocks range from 0.01 to 0.95, suggesting their metamorphic origin (Teipel et al., 2004). The obtained U-Pb and ^{40}Ar-^{39}Ar ages from the different mineral phases (zircon, titanite and amphibole) with different isotopic closure temperatures for the metamorphic sole rocks in the three regions are identical within analytical uncertainty (1σ; Table 6; Fig. 14). Radiogenic Pb* closure temperature was constrained as 550–650 °C for

titanite (Cherniak, 1993). Radiogenic $^{40}Ar^*$ closure temperature for amphibole was constrained as 510 ± 25 °C (Harrison, 1982). *P-T* estimates for the metamorphic sole beneath the Beyşehir-Hoyran Nappes were constrained as 550–600 °C and <5 kbar by Çelik and Delaloye (2006) in the Gencek (Konya) area, and 630–770 °C and 6 ± 1.5 kbar by Elitok and Drüppel (2008) in the Şarkikaraağaç-Madenli (Isparta) area. *P-T* calculations in this study are ~5.7 ± 1.0 kbar and 570 ± 40 °C for the Gencek region and ~6.7 ± 1.3 kbar and 590 ± 110 °C for the Şarkikaraağaç-Madenli region. The obtained temperature range offers considerable compatibility with the zircon recrystallization or new zircon growth during subduction-related metamorphism. The metamorphic soles yielded constant and well-constrained $^{40}Ar/^{39}Ar$ plateau ages for three samples. Çelik and Delaloye (2006) also documented well-constrained ^{40}Ar-^{39}Ar plateau ages of 90.9 ± 1.3 Ma and 91.5 ± 1.9 Ma from amphiboles extracted from the metamorphic sole rocks in the Gencek (Konya) area (Table 6). This may suggest that they did not experience any reheating event over 550 °C after their initial formation. On the other hand, one sample (G14-4) from the Gencek (Konya) area displays $^{40}Ar^*$ loss at 48 Ma (mid-Eocene). When all the $^{40}Ar/^{39}Ar$ ages are considered, this sample records the effects of overprinting low-grade metamorphic conditions that followed the high-grade Cretaceous crystallization event. Since the Late Cretaceous and mid-Eocene southward emplacement of Tauride thrust sheets in the Beyşehir-Hoyran Nappes is well documented (Mackintosh and Robertson, 2013), the second stage of thrusting that buried the ophiolite-related rocks in mid-Eocene time could be interpreted as the main cause for $^{40}Ar^*$ loss. Overall identical U-Pb and ^{40}Ar-^{39}Ar ages of different mineral phases with different closure temperatures (~900–500 °C) suggest that the metamorphic sole must have cooled very rapidly, similar to the tectonically overlying oceanic crustal rocks. Therefore, all the obtained geochronological data should be interpreted as the crystallization age of the metamorphic sole, which marks the timing of intra-oceanic subduction within the Inner Tauride Ocean.

Alternative Models for Genesis of Ophiolite and Metamorphic Sole

REE patterns and trace-element plots of the isolated dikes cutting the mantle tectonites resemble tholeiitic island-arc basalts. Therefore, we favor a suprasubduction zone model because it more simply explains both the geochemical constraints and our new U-Pb data from the ophiolite and metamorphic sole. Pearce et al. (1984) proposed that suprasubduction zone–type geochemical signatures result from the remelting of already depleted mantle sources that had been subjected to previous MORB extraction, as a result of the addition of slab-derived fluids. Suprasubduction zone ophiolites are thought to form at spreading centers in a forearc during the subduction initiation process (Dewey and Casey, 2011; Shervais, 2001; Stern, 2004; Stern and Bloomer, 1992; Stern et al., 2012). Transform faults or fracture zones, separating oceanic lithosphere of different ages and densities, are the most plausible sites of subduction initiation normal to mid-ocean ridges (Casey and Dewey, 1984; Dewey and Casey, 2011; Hawkins et al., 1984; Leitch, 1984; Stern and Bloomer, 1992). Dewey and Casey (2011) proposed a model involving a ridge-trench-trench (RTT) triple junction with the ridge between the upper plates. They suggested that such a plate geometry developed by the conversion of a transform/fracture zone to a subduction zone due to plate reorganization. Arc-parallel spreading and lithospheric cooling and thickening generate an ophiolitic forearc with arc-normal dikes, similar to evidence from the Philippine Sea in the western and southwestern Pacific Ocean (Fig. 15A). Recently, Maffione et al. (2015) proposed that extensional detachment faults adjacent to slow-spreading ridges may provide ideal conditions to nucleate new subduction zones parallel to the spreading ridges. Detachment faults may become suitable areas for subduction initiation because of widespread occurrences of serpentine and talc due to hydrothermal alteration (Maffione et al., 2015). They documented geochemical, tectonic, and paleomagnetic evidence from the Jurassic ophiolites of Albania and Greece for a subduction zone formed in the western Neotethys parallel to a spreading ridge along an oceanic detachment fault. However, most ultramafic rocks in ophiolite complexes were slightly serpentinized in oceanic settings, and serpentinization was mainly a postobduction process (Dewey and Casey, 2011). Gnos and Peters (1993) suggested that another weak zone for the site of subduction initiation within the Tethyan oceanic lithosphere could have been the feeding zone of a seamount.

The metamorphic sole was developed in the subducting mafic oceanic crust at temperatures of 850–900 °C and then detached from the subducting slab to be attached to the base of the forearc ophiolite before emplacement onto a continental margin (Dewey and Casey, 2011). Many soles display inverted metamorphic field gradients (Spray, 1984). The inverted temperature anomaly responsible for the high-grade metamorphism of the sole decays quickly (<2 m.y.) as subduction continues (Hacker, 1990, 1991; Hacker et al., 1996; Peacock, 1988). Thus, the high-grade metamorphism of the sole can occur only at the inception of subduction because the hanging wall would be too cold to cause high-grade metamorphism thereafter (Jamieson, 1986; Malpas, 1979; Spray, 1984; Wakabayashi and Dilek, 2000, 2003; Williams and Smyth, 1973).

The temporal relationships of metamorphic soles and suprasubduction zone–type ophiolite formation, and the exhumation of the metamorphic sole and its attachment to the base of the overriding plate in intra-oceanic subduction zones have been topics of debate in recent years. Dewey and Casey (2013) proposed an integrated model for the sole and the obduction of the Early Ordovician Bay of Islands ophiolite complex (Fig. 15B). The metamorphic sole at the base of the ophiolite was generated, roughly synchronously with the ophiolite, by the metamorphism of MORB mafic rocks in the subforearc subduction channel as a natural consequence of the dynamothermal metamorphism of the subducting oceanic crust below the subridge asthenosphere of the forearc in the descending slab at ~10 kbar, and it was then quickly attached to the base of the overlying ophiolite during slab flattening. The slab flattening resulted from the forearc mantle wedge thinning by shallowing of the subduction zone dip during arc-continent collision (Fig. 15B). Dewey and Casey (2011) stated that the asthenospheric mantle below the ridge at the RTT junction above 900 °C can be thinned. Subsequently, van Hinsbergen et al. (2015) proposed a similar model to Dewey and Casey (2013), namely, suprasubduction zone spreading, metamorphic sole formation, mantle wedge volume decrease, slab flattening, metamorphic sole attachment to the base of the suprasubduction zone lithosphere, and subsequent mafic dike emplacement. Their model involved extensional detachment faults adjacent to slow-spreading ridges for nucleating the new subduction zone (Fig. 15C). In contrast, in Oman, the granulite-amphibolite facies sole rocks were exhumed up to shallower mantle levels and were welded onto the ophiolite prior to obduction (Searle and Cox, 2002; Cowan et al., 2014; Searle at al., 2015). Obduction processes include rapid return ductile flow back up the same subduction zone, transition from ductile shearing to brittle thrusting, and finally transition to thin-skinned thrust imbrication (Fig. 15D). Wakabayashi and Dilek (2000) also stated that exhumation of the sole occurred in a narrow channel along the subduction plate contact. Similarly, Rioux et al. (2016) calculated density differences between the metamorphic sole (granulite-amphibolite–facies) rocks and the overlying mantle wedge. They reported that

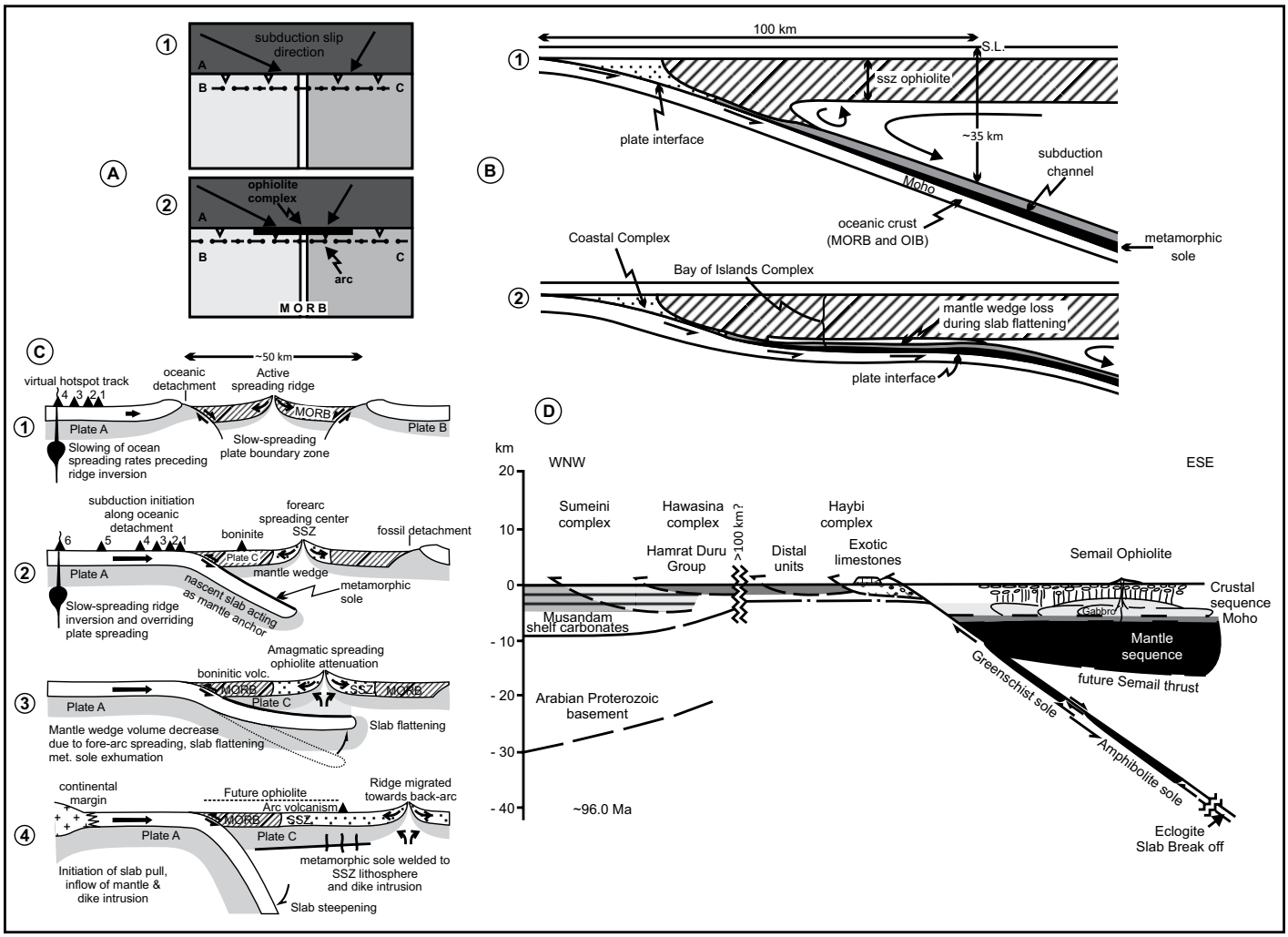

Figure 15. Alternative models for subduction initiation, genesis, and emplacement of forearc ophiolite–metamorphic sole pair. Please see text for discussion. (A1) Plan view of ridge-trench-trench (RTT) triple junction and (A2) ophiolite genesis (from Dewey and Casey, 2011). (B) Schematic sections for the tectonic setting of the Bay of Islands ophiolite and underlying metamorphic sole (simplified from Dewey and Casey, 2013). S.L.—sea level; ssz—suprasubduction zone; MORB—mid-ocean-ridge basalt; OIB—oceanic-island basalt. (C) Cross-sectional evolution of intra-oceanic subduction initiation, genesis of suprasubduction zone (SSZ) ophiolite–metamorphic sole pair, and subsequent dike emplacement (from van Hinsbergen et al., 2015). (D) Model for the formation and emplacement of the Semail ophiolite in the northern Oman mountains, showing the relative positions of the ophiolite and the metamorphic sole during the Cenomanian (from Cowan et al., 2014; Searle et al., 2015).

the garnet granulites were at least 50–75 kg/m^3 less dense than the overlying hydrated mantle wedge. Moreover, the density difference would have increased as the metamorphic rocks rose to lower pressures and underwent retrograde reactions at amphibolite-facies conditions. This suggests that metamorphic sole rocks could be exhumed by buoyancy along the subduction channel (Rioux et al., 2016).

Proposed Tectonic Model

When the previously published geochronological (^{40}Ar-^{39}Ar) and geochemical data on the Tauride ophiolites and the new data from this study for the Beyşehir-Hoyran Nappes are considered together, the genesis of oceanic lithosphere, metamorphic sole formation, and postmetamorphic dike emplacement may well be reconciled by a suprasubduction zone model, including subduction initiation and rollback processes in the Inner Tauride Ocean during the Late Cretaceous. The evidence for very rapid cooling of the oceanic crust and the metamorphic sole rocks in the Beyşehir-Hoyran ophiolite suggests that the sole rocks returned up the subduction channel, cooled, and were juxtaposed with the base of the ophiolite soon after peak metamorphism. An evolutionary model is suggested in Figure 16 and described as follows. (1) Subduction initiation would have started either along a fracture zone or at an active spreading ridge within the Inner Tauride Ocean, or at a trench where old, cold Triassic–Jurassic seafloor rocks were being subducted. There is no structural evidence for transform faulting. The site of initiation of subduction cannot have been at an active spreading ridge in the Late Cretaceous because the protoliths of the metamorphic sole rocks have compositions different from lavas in the upper part of overriding suprasubduction zone ophiolite. In the Beyşehir-Hoyran Nappes,

mainly OIB-like alkaline volcanic rocks and associated sediments were accreted to the base of the overriding oceanic plate and were metamorphosed under amphibolite-facies conditions (5–6 kbar and 600–700 °C) at ca. 92–90 Ma. We therefore reject both the transform fault setting and the active spreading ridge setting for this particular ophiolite. However, the site of subduction initiation in the Inner Tauride Ocean would have been close to a seamount where old, cold Triassic–Jurassic seafloor rocks were being subducted northward beneath the Beyşehir-Hoyran ophiolite (Fig. 16A). (2) At the same time as the subduction initiation and metamorphic sole formation, suprasubduction zone–type oceanic crust formed in the forearc region of the upper plate (92–90 Ma). The U-Pb and ^{40}Ar-^{39}Ar ages of mineral phases with different closure temperatures (~900–500 °C) from the metamorphic sole rocks are almost identical and overlapping within one standard deviation, suggesting that the metamorphic sole was cooled very rapidly. This suggests that metamorphic sole rocks could have been exhumed by buoyancy along the subduction channel and then detached from the subducting slab to be attached to the hanging-wall plate (forearc ophiolite) soon after peak metamorphism (Fig. 16B). (3) Following the attachment of the metamorphic sole to the overriding plate, the old and dense lithosphere sank into the asthenosphere (i.e., rolled back) and left a gap that was filled by rapid spreading at the leading edge of the overriding plate. Decompression and contribution of fluids released from the subducted slab lowered the solidus of the mantle wedge and caused extensive melting of the shallow asthenosphere. Crustal formation was fed by melts, including both boninitic (high-Mg andesites) and island-arc tholeiitic magmas, leaving a refractory harzburgitic mantle tectonite (Stern and Bloomer, 1992). Evidence for boninitic magma genesis has been documented for the Tethyan ophiolites in Turkey (Bağcı et al., 2008; Bağcı and Parlak, 2009; Kavak et al., 2017). (4) During this phase, postmetamorphic isolated dikes exhibiting island-arc tholeiite and OIB geochemical affinity intruded the metamorphic sole and the overlying oceanic lithosphere (92–90 Ma) in the Beyşehir-Hoyran ophiolite (Fig. 16C). The mantle tectonites and the metamorphic soles in the Tauride ophiolites are crosscut by numerous isolated diabase dikes at different structural levels. The dikes are not deformed and exhibit sharp boundaries with host units. They are generally 30 cm to 3 m in thick and at least 10 m in length. This suggests that the dike emplacement occurred near the end of deformation or that the locus of deformation shifted after dike emplacement. In two areas along the Tauride belt, the Pozantı-Karsantı (Aladağ) and the Lycian ophiolites, the contact between the metamorphic sole and the overlying serpentinized harzburgites was intruded by a thick mafic dike (up to 7–8 m) that postdated intra-oceanic metamorphism and high-temperature ductile deformation. This contact is interpreted as an intra-oceanic decoupling surface along which volcanics from the upper levels of the downgoing plate were metamorphosed to amphibolite facies and accreted to the base of the hanging-wall plate (Parlak, 2016). The isolated dikes were derived mainly from tholeiitic magma and, to a lesser extent, from alkaline magma, suggesting that an enriched magma source invaded the gap between the overriding and subducting plates due to rollback process. Small-scale dioritic to tonalitic pods and dikes (15 cm × 5 cm) from the Sumeini and Wadi Tayin soles in the Oman ophiolite have been documented

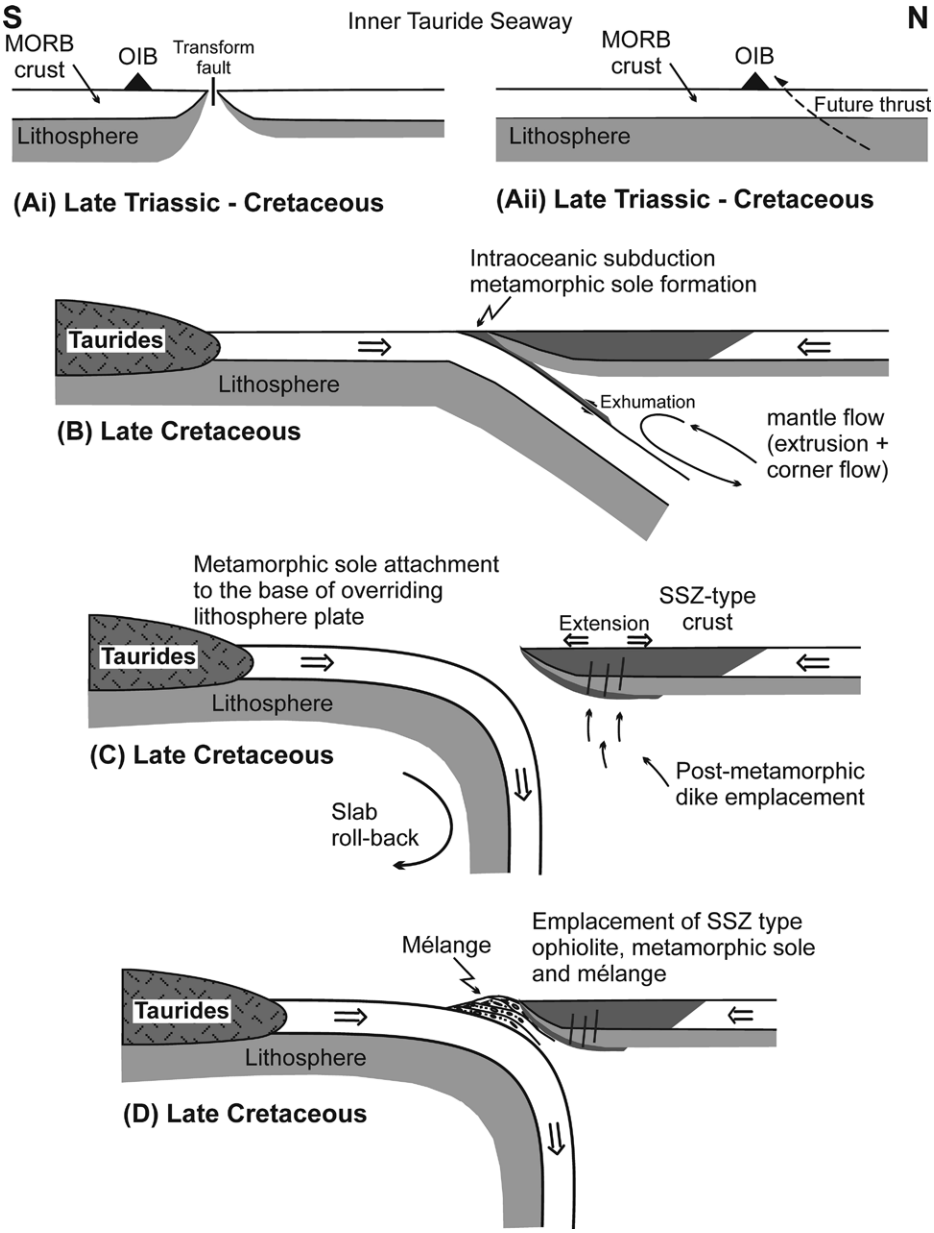

Figure 16. Proposed tectonic model for the genesis of the ophiolites and metamorphic soles and subsequent dike emplacement in the Inner Tauride Ocean (modified from Parlak, 2016). MORB—mid-ocean-ridge basalt; OIB—oceanic-island basalt; SSZ—suprasubduction zone.

and interpreted as either small-volume high-Si intrusions formed by melting of an amphibolite source during peak metamorphism (Cowan et al., 2014; Searle and Malpas, 1980, 1982; Searle and Cox, 1999) or low-Si mafic melts derived from cumulates (Rioux et al., 2016). The postmetamorphic isolated dikes are not observed in the ophiolitic mélange, suggesting they were intruded prior to mélange formation and subsequent to ophiolite emplacement onto the Tauride platform (Fig. 16D).

CONCLUSIONS

(1) The temporal relations of the metamorphic sole and overlying ophiolite in the Beyşehir-Hoyran Nappes are well constrained despite different isotopic blocking temperatures of mineral phases (zircon, titanite, and amphibole) with different isotopic techniques (U-Pb and ^{40}Ar-^{39}Ar), suggesting very rapid cooling of the oceanic crust and the metamorphic sole.

(2) The crystallization age of the ophiolitic rocks is constrained at around 92–90 Ma and was in part synchronous with the formation of the metamorphic sole (ca. 92–90 Ma) along the emplacement thrust. These new findings confirm the suprasubduction zone origin of the Beyşehir-Hoyran ophiolite within the Inner Tauride Ocean during the Late Cretaceous.

(3) The isolated dikes cutting the mantle tectonites in the Şarkikaraağaç and Gencek regions were derived from island-arc tholeiitic magmas, indicating their subduction-related origin. In contrast, the postmetamorphic isolated dike cutting the metamorphic sole to the north of Lake Beyşehir (Madenli) was derived from an enriched mantle source. The late-stage dike with enriched composition is interpreted as being due to rollback process or having been derived from local fractures or tears in the subducting plate rather than large-scale break-off, because slab break-off would produce much greater volumes of enriched magma than that contained in these late-stage isolated dikes.

(4) The site of initiation of intra-oceanic subduction cannot have been at a mid-oceanic ridge because the protoliths of the amphibolites in the metamorphic sole would have to be similar to the suprasubduction zone-type ophiolitic volcanic rocks. Immobile trace-element geochemistry shows that they were mainly derived from seamount-type alkaline basalts. The site of subduction initiation in the Inner Tauride Ocean would have been close to a seamount where old, cold Triassic–Jurassic seafloor rocks were being subducted northward beneath the Beyşehir-Hoyran ophiolite.

(5) The similar U-Pb crystallization and ^{40}Ar/^{39}Ar cooling ages from the ophiolite crust and metamorphic sole may suggest that the sole rocks returned up the subduction channel, cooled, and were juxtaposed with the base of the ophiolite soon after peak metamorphism but before postmetamorphic dike intrusion.

(6) The new results from zircon U-Pb dating of amphibolites from metamorphic soles suggest that zircon minerals could be modified or reset in fluid-rich subduction-related environments at temperatures of ~500–550 °C.

(7) Subduction initiation started at around 92 Ma, and final emplacement of the subduction-accretion complex onto the Tauride platform ended by the Maastrichtian (Andrew and Robertson, 2002), suggesting that the entire obduction history of the Beyşehir-Hoyran ophiolite lasted ~20 m.y.

ACKNOWLEDGMENTS

Alastair Robertson, Benxun Su, and Associate Editor Erdin Bozkurt are thanked for their constructive and very valuable comments that improved the quality of the paper. We would like to thank Seher Kuru and Aynur Gürbüz for their help during cathodoluminescence imaging of zircons at Mersin University. Güzide Önal is thanked for drawing the figures. This work was funded by TÜBİTAK (Project no. 113Y412) awarded to O. Parlak, and Chinese National Natural Science Foundation grant 91755213, awarded to T. Kusky. O. Parlak acknowledges the Open Fund (GPMR201702) of State Key Lab of Geological Processes and Mineral Resources, China University of Geosciences, Wuhan for additional support.

REFERENCES CITED

Alabaster, T., Pearce, J.A., and Malpas, J., 1982, The volcanic stratigraphy and petrogenesis of the Oman ophiolite complex: Contributions to Mineralogy and Petrology, v. 81, p. 168–183, https://doi.org/10.1007/BF00371294.

Alparslan, G., and Dilek, Y., 2018, Seafloor spreading structure, geochronology, and tectonic evolution of the Küre ophiolite, Turkey: A Jurassic continental backarc basin oceanic lithosphere in southern Eurasia: Lithosphere, v. 10, p. 14–34, https://doi.org/10.1130/L641.1.

Al-Riyami, K., Robertson, A.H.F., Xenophontos, C., Danelian, T., and Dixon, J.E., 2002, Origin and emplacement of the Late Cretaceous Baer-Bassit ophiolite and its metamorphic sole in NW Syria: Lithos, v. 65, p. 225–260, https://doi.org/10.1016/S0024-4937(02)00167-6.

Andrew, T., and Robertson, A.H.F., 2002, The Beyşehir-Hoyran-Hadim Nappes: Genesis and emplacement of Mesozoic marginal and oceanic units of the northern Neotethys in southern Turkey: Journal of the Geological Society [London], v. 159, p. 529–543, https://doi.org/10.1144/0016-764901-157.

Arculus, R.J., and Powel, R., 1986, Source component mixing in the regions of arc magma generation: Journal of Geophysical Research, v. 91, p. 5913–5926, https://doi.org/10.1029/JB091iB06p05913.

Bağcı, U., and Parlak, O., 2009, Petrology of the Tekirova (Antalya) ophiolite (southern Turkey): Evidence for diverse magma generations and their tectonic implications during Neotethyan subduction: International Journal of Earth Sciences, v. 98, p. 387–405, https://doi.org/10.1007/s00531-007-0242-7.

Bağcı, U., Parlak, O., and Höck, V., 2008, Geochemistry and tectonic environment of diverse magma generations forming the crustal units of the Kızıldağ (Hatay) ophiolite, southern Turkey: Turkish Journal of Earth Sciences, v. 17, p. 43–71.

Beccaluva, L., Coltorti, M., Giunta, G., and Siena, F., 2004, Tethyan vs. Cordilleran ophiolites: A reappraisal of distinctive tectonomagmatic features of suprasubduction complexes in relation to the subduction mode: Tectonophysics, v. 393, p. 163–174, https://doi.org/10.1016/j.tecto.2004.07.034.

Beccaluva, L., Coltorti, M., Saccani, E., and Siena, F., 2005, Magma generation and crustal accretion as evidenced by supra-subduction ophiolites of the Albanide-Hellenide Subpelagonian zone: The Island Arc, v. 14, p. 551–563, https://doi.org/10.1111/j.1440-1738.2005.00483.x.

Bloomer, S.H., and Hawkins, J.W., 1983, Gabbroic and ultramafic rocks from the Mariana Trench. Part 2, *in* Hayes, D.E., ed., The Tectonic Evolution of Southeast Asian Seas and Islands: American Geophysical Union Geophysical Monograph 27, p. 294–317.

Boudier, F., Ceuleneer, G., and Nicolas, A., 1988, Shear zones, thrusts and related magmatism in the Oman ophiolite: Initiation of thrusting on an oceanic ridge: Tectonophysics, v. 151, p. 275–296, https://doi.org/10.1016/0040-1951(88)90249-1.

Casey, J.F., and Dewey, J.F., 1984, Initiation of subduction zones, *in* Gass, I.G., Lippard, S.J., and Shelton, A.W., eds., Ophiolites and Oceanic Lithosphere: Geological Society [London] Special Publication 13, p. 269–290.

Çelik, Ö.F., 2007, Metamorphic sole rocks and their mafic dykes in the eastern Tauride belt ophiolites (southern Turkey): Implications for OIB type magma generation following slab break-off: Geological Magazine, v. 144, p. 849–866, https://doi.org/10.1017/S0016756807003573.

Çelik, Ö.F., and Chiaradia, M., 2008, Geochemical and petrological aspects of dyke intrusions in the Lycian ophiolites (SW Turkey): A case study for the dyke emplacement along the Tauride belt ophiolites: International Journal of Earth Sciences, v. 97, p. 1151–1164, https://doi.org/10.1007/s00531-007-0204-0.

Çelik, Ö.F., and Delaloye, M., 2003, Origin of metamorphic soles and their post-kinematic mafic dyke swarms in the Antalya and Lycian ophiolites, SW Turkey: Geological Journal, v. 38, p. 235–256, https://doi.org/10.1002/gj.954.

Çelik, Ö.F., and Delaloye, M., 2006, Characteristics of ophiolite-related metamorphic rocks in the Beyşehir ophiolitic mélange (Central Taurides, Turkey), deduced from whole rock and mineral chemistry: Journal of Asian Earth Sciences, v. 26, p. 461–476, https://doi.org/10.1016/j.jseaes.2004.10.008.

Çelik, Ö.F., Delaloye, M., and Feraud, G., 2006, Precise ^{40}Ar-^{39}Ar ages from the metamorphic sole rocks of the Tauride belt ophiolites, southern Turkey: Implications for the rapid cooling history: Geological Magazine, v. 143, p. 213–227, https://doi.org/10.1017/S0016756805001524.

Çelik, Ö.F., Marzoli, A., Marschik, R., Chiaradia, M., Neubauer, N., and Öz, İ., 2011, Early-Middle Jurassic intraoceanic subduction in the İzmir-Ankara-Erzincan Ocean, northern Turkey: Tectonophysics, v. 509, p. 120–134, https://doi.org/10.1016/j.tecto.2011.06.007.

Cherniak, D.J., 1993, Lead diffusion in titanite and preliminary results on the effects of radiation damage on Pb transport: Chemical Geology, v. 110, p. 177–194, https://doi.org/10.1016/0009-2541(93)90253-F.

Cherniak, D.J., and Watson, E.B., 2001, Pb diffusion in zircon: Chemical Geology, v. 172, p. 5–24, https://doi.org/10.1016/S0009-2541(00)00233-3.

Corfu, F., Hanchar, J.M., Hoskin, P.W.O., and Kinny, P., 2003, Atlas of zircon textures: Reviews in Mineralogy and Geochemistry, v. 53, p. 469–500, https://doi.org/10.2113/0530469.

Cowan, R.J., Searle, M.P., and Waters, D.J., 2014, Structure of the metamorphic sole to the Oman ophiolite, Sumeini Window and Wadi Tayyin: Implications for ophiolite obduction processes, *in* Rollinson, H.R., Searle, M.P., Abbasi, I.A., Al-Lazki, A., and Al Kindi, M.H., eds., Tectonic Evolution of the Oman Mountains: Geological Society [London] Special Publication 392, p. 155–175.

Dewey, J.F., and Casey, J.F., 2011, The origin of obducted large-slab ophiolite complexes, *in* Brown, D., and Ryan, P.D., eds., Arc-Continent Collision: Frontiers in Earth Sciences: Berlin, Springer-Verlag, p. 431–444.

Dewey, J.F., and Casey, J.F., 2013, The sole of an ophiolite: The Ordovician Bay of Islands Complex, Newfoundland: Journal of the Geological Society [London], v. 170, p. 715–722, https://doi.org/10.1144/jgs2013-017.

Dilek, Y., and Flower, M.F.J., 2003, Arc-trench rollback and forearc accretion: 2. A model template for ophiolites in Albania, Cyprus, and Oman, *in* Dilek, Y., and Robinson P.T., eds., Ophiolites in Earth History: Geological Society [London] Special Publication 218, p. 43–68.

Dilek, Y., and Thy, P., 2006, Age and petrogenesis of plagiogranite intrusions in the Ankara mélange, central Turkey: The Island Arc, v. 15, p. 44–57, https://doi.org/10.1111/j.1440-1738.2006.00522.x.

Dilek, Y., and Thy, P., 2009, Island arc tholeiite to boninitic melt evolution of the Cretaceous Kizildag (Turkey) ophiolite: Model for multi-stage early arc-forearc magmatism in Tethyan subduction factories: Lithos, v. 113, no. 1-2, p. 68–87.

Dilek, Y., and Whitney, D.L., 1997, Counterclockwise *P-T-t* trajectory from the metamorphic sole of a Neo-Tethyan ophiolite (Turkey): Tectonophysics, v. 280, p. 295–310, https://doi.org/10.1016/S0040-1951(97)00038-3.

Dilek, Y., Thy, P., Hacker, B.R., and Grundvig, S., 1999, Structure and petrology of Tauride ophiolites and mafic dyke intrusions (Turkey): Implications for the Neotethyan ocean: Geological Society of America Bulletin, v. 111, p. 1192–1216, https://doi.org/10.1130/0016-7606(1999)111<1192:SAPOTO>2.3.CO;2.

Dilek, Y., Furnes, H., and Shallo, M., 2008, Geochemistry of the Jurassic Mirdita ophiolite (Albania) and the MORB to SSZ evolution of a marginal basin oceanic crust: Lithos, v. 100, p. 174–209, https://doi.org/10.1016/j.lithos.2007.06.026.

Dunkl, I., Mikes, T., Simon, K., and von Eynatten, H., 2008, Brief introduction to the Windows program Pepita: Data visualization, and reduction, outlier rejection, calculation of trace element ratios and concentrations from LA-ICP-MS data, *in* Sylvester, P., ed., Laser Ablation ICP-MS in the Earth Sciences: Current Practices and Outstanding Issues: Quebec City, Canada, Mineralogical Association of Canada, p. 334–340.

Elitok, Ö., and Drüppel, K., 2008, Geochemistry and tectonic significance of metamorphic sole rocks beneath the Beyşehir-Hoyran ophiolite (SW-Turkey): Lithos, v. 100, p. 322–353, https://doi.org/10.1016/j.lithos.2007.06.022.

Floyd, P.A., and Winchester, J.A., 1978, Identification and discrimination of altered and metamorphosed volcanic rocks using immobile elements: Chemical Geology, v. 21, p. 291–306, https://doi.org/10.1016/0009-2541(78)90050-5.

Frei, D., and Gerdes, A., 2009, Precise and accurate in situ U-Pb dating of zircon with high sample throughput by automated LA-SF-ICP-MS: Chemical Geology, v. 261, no. 3-4, p. 261–270, https://doi.org/10.1016/j.chemgeo.2008.07.025.

Geisler, T., Ulonska, M., Schleicher, H., Pidgeon, R.T., and van Bronswijk, W., 2001, Leaching and differential recrystallization of metamict zircon under experimental hydrothermal conditions: Contributions to Mineralogy and Petrology, v. 141, p. 53–65, https://doi.org/10.1007/s004100000202.

Gill, J.B., 1981, Orogenic Andesites and Plate Tectonics (Minerals, Rocks and Mountains Volume 16): Berlin, Springer-Verlag, 390 p., https://doi.org/10.1007/978-3-642-68012-0.

Gnos, E., and Peters, T., 1993, K-Ar ages of the metamorphic sole of the Semail ophiolite: Implications for cooling history: Contributions to Mineralogy and Petrology, v. 113, p. 325–332, https://doi.org/10.1007/BF00286925.

Göncüoğlu, M.C., Turhan, N., Şentürk, K., Özcan, A., Uysal, S., and Yalınız, M.K., 2000, A geotraverse across northwestern Turkey: Tectonic units of the Sakarya region and their tectonic evolution, *in* Bozkurt, E., Winchester, J.A., and Piper, J.D.A., eds., Tectonics and Magmatism in Turkey and the Surrounding Area: Geological Society [London] Special Publication 173, p. 193–161.

Göncüoğlu, M.C., Yalınız, M.K., and Tekin, U.K., 2006, Geochemistry, tectono-magmatic discrimination and radiolarian ages of basic extrusives from the İzmir-Ankara suture belt (NW Turkey): Time constraints for the Neotethyan evolution: Ofioliti, v. 31, p. 25–38.

Göncüoğlu, M.C., Sayıt, K., and Tekin, U.K., 2010, Oceanization of the northern Neotethys: Geochemical evidence from ophiolitic mélange basalts within the İzmir-Ankara suture belt, NW Turkey: Lithos, v. 116, p. 175–187, https://doi.org/10.1016/j.lithos.2010.01.007.

Gutnic, M., Monod, O., Poisson, A., and Dumont, J.F., 1979, Geologie des Taurides Occidentales (Turquie): Memories de la Société Géologique de France 137, 112 p.

Hacker, B.R., 1990, Simulation of the metamorphic and deformational history of the metamorphic sole of the Oman ophiolite: Journal of Geophysical Research, v. 95, p. 4895–4907, https://doi.org/10.1029/JB095iB04p04895.

Hacker, B.R., 1991, The role of deformation in the formation of metamorphic field gradients: Ridge subduction beneath the Oman ophiolite: Tectonics, v. 10, p. 455–473, https://doi.org/10.1029/90TC02779.

Hacker, B.R., 1994, Rapid emplacement of young oceanic lithosphere: Argon geochronology of the Oman ophiolites: Science, v. 265, p. 1563–1565, https://doi.org/10.1126/science.265.5178.1563.

Hacker, B.R., and Gnos, E., 1997, The conundrum of Semail: Explaining the metamorphic history: Tectonophysics, v. 279, p. 215–226, https://doi.org/10.1016/S0040-1951(97)00114-5.

Hacker, B.R., Mosenfelder, J.L., and Gnos, E., 1996, Rapid emplacement of the Oman ophiolite: Thermal and geochronological constraints: Tectonics, v. 15, p. 1230–1247, https://doi.org/10.1029/96TC01973.

Hammarstrom, J.M., and Zen, E.-A., 1986, Aluminium in hornblende: An empirical igneous geobarometer: The American Mineralogist, v. 71, p. 1297–1313.

Harrison, T.M., 1982, Diffusion of ^{40}Ar in hornblende: Contributions to Mineralogy and Petrology, v. 78, p. 324–331, https://doi.org/10.1007/BF00398927.

Hart, S.R., Erlank, A.J., and Kable, E.J.D., 1974, Sea floor basalt alteration: Some chemical and Sr isotopic effects: Contributions to Mineralogy and Petrology, v. 44, p. 219–230, https://doi.org/10.1007/BF00413167.

Hawkins, J.W., Bloomer, S.H., Evans, C.A., and Melchior, J.T., 1984, Evolution of intra-oceanic arc-trench systems: Tectonophysics, v. 102, p. 175–205, https://doi.org/10.1016/0040-1951(84)90013-1.

Holland, T., and Blundy, J., 1994, Non-ideal interactions in calcic amphiboles and their bearing on amphibole-plagioclase thermometry: Contributions to Mineralogy and Petrology, v. 116, p. 433–447, https://doi.org/10.1007/BF00310910.

Hollister, L.S., Grissom, G.C., Peters, E.K., Stowell, H.H., and Sissom, V.B., 1987, Confirmation of the empirical correlation of Al in hornblende with pressure of solidification of calc alkaline plutons: The American Mineralogist, v. 72, p. 231–239.

Hoskin, P.W.O., and Black, L.P., 2000, Metamorphic zircon formation by solid-state recrystallization of protolith igneous zircon: Journal of Metamorphic Geology, v. 18, p. 423–439, https://doi.org/10.1046/j.1525-1314.2000.00266.x.

Hoskin, P.W.O., and Schaltegger, U., 2003, The composition of zircon and igneous and metamorphic petrogenesis, *in* Hanchar, J.M., and Hoskin, P.W.O., eds., Zircon: Mineralogical Society of America Reviews in Mineralogy and Geochemistry 53, p. 27–62, https://doi.org/10.1515/9781501509322-005.

Humphris, S.E., and Thompson, G., 1978, Trace element mobility during hydrothermal alteration of oceanic basalts: Geochimica et Cosmochimica Acta, v. 42, p. 127–136, https://doi.org/10.1016/0016-7037(78)90222-3.

Jackson, S.E., Pearson, N.J., Griffin, W.L., and Belousova, E.A., 2004, The application of laser ablation–inductively coupled plasma–mass spectrometry to in situ U-Pb zircon geochronology: Chemical Geology, v. 211, p. 47–69, https://doi.org/10.1016/j.chemgeo.2004.06.017.

Jamieson, R.A., 1980, Formation of metamorphic aureoles beneath ophiolites: Evidence from the St. Anthony Complex, Newfoundland: Geology, v. 8, p. 150–154, https://doi.org/10.1130/0091-7613(1980)8<150:FORABO>2.0.CO;2.

Jamieson, R.A., 1986, PT paths from high temperature shear zones beneath ophiolites: Journal of Metamorphic Geology, v. 4, p. 3–22, https://doi.org/10.1111/j.1525-1314.1986.tb00335.x.

Johnson, M.C., and Rutherford, M.J., 1989, Experimental calibration of the aluminum-in-hornblende geobarometer with application to Long Valley caldera (California) volcanic rocks: Geology, v. 17, no. 9, p. 837–841, https://doi.org/10.1130/0091-7613(1989)017<0837:ECOTAI>2.3.CO;2.

Kamenetsky, V.S., Sobolev, A.V., Eggins, S.M., Crawford, A.J., and Arculus, R.J., 2002, Olivine-enriched melt inclusions in chromites from low-Ca boninites, Cape Vogel, Papua New Guinea: Evidence for ultramafic primary magma, refractory mantle source and enriched components: Chemical Geology, v. 183, p. 287–303, https://doi.org/10.1016/S0009-2541(01)00380-1.

Karaoğlan, F., Parlak, O., Klötzli, U., Thöni, M., and Koller, F., 2012, U-Pb and Sm-Nd geochronology of the ophiolites from the SE Turkey: Implications for the Neotethyan evolution: Geodinamica Acta, v. 25, p. 146–161, https://doi.org/10.1080/09853111.2013.858948.

Karaoğlan, F., Parlak, O., Klötzli, U., Thöni, M., and Koller, F., 2013a, U-Pb and Sm-Nd geochronology of the Kızıldağ (Hatay, Turkey) ophiolite: Implications for the timing and duration of suprasubduction zone type oceanic crust formation in the southern Neotethys: Geological Magazine, v. 150, p. 283–299, https://doi.org/10.1017/S0016756812000477.

Karaoğlan, F., Parlak, O., Klötzli, U., Koller, F., and Rızaoğlu, T., 2013b, Age and duration of intraoceanic arc volcanism built on a suprasubduction zone type oceanic crust in southern Neotethys, SE Anatolia: Geoscience Frontiers, v. 4, p. 399–408, https://doi.org/10.1016/j.gsf.2012.11.011.

Kavak, K.Ş., Parlak, O., and Temiz, H., 2017, Geochemical characteristics of ophiolitic rocks from the southern margin of the Sivas basin and their implications for the Inner Tauride Ocean, central-eastern Turkey: Geodinamica Acta, v. 29, p. 160–180, https://doi.org/10.1080/09853111.2017.1359773.

Koçyiğit, A., 1984, Tectonostratigraphic characteristics of Hoyran Lake region (Isparta Bend), *in* Tekeli, O., and Göncüoğlu, C., eds., Proceedings of the International Symposium on the Geology of the Taurus Belt: Ankara, Turkey, General Directorate of Mineral Research and Exploration (MTA), p. 53–67.

Koglin, N., 2008, Geochemistry, Petrogenesis and Tectonic Setting of Ophiolites and Mafic-Ultramafic Complexes in the Northeastern Aegean Region: New Trace-Element, Isotopic and Age Constraints [Ph.D. thesis]: Mainz, Germany, Johannes Gutenberg University, 136 p.

Koglin, N., Kostopoulos, D., and Reichmann, T., 2009, Geochemistry, petrogenesis and tectonic setting of the Samothraki mafic suite, NE Greece: Trace-element, isotopic and zircon age constraints: Tectonophysics, v. 473, p. 53–68, https://doi.org/10.1016/j.tecto.2008.10.028.

Konstantinou, A., Wirth, K.R., and Vervoort, J., 2007, U-Pb isotopic dating of Troodos plagiogranite, Cyprus, by LA-ICP-MS: Geological Society of America Abstracts with Programs, v. 39, no. 6, p. 338.

Leake, B.E., Woolley, A.R., Arps, C.E.S., Birch, W.D., Gilbert, M.C., Grice, J.D., et al., 1997, Nomenclature of amphiboles: Report of the Subcommittee on Amphiboles of the International Mineralogical Association, Commission on New Minerals and Mineral Names: The American Mineralogist, v. 82, p. 1019–1037.

Leitch, E.C., 1984, Island arc elements and arc related ophiolites: Tectonophysics, v. 106, p. 177–203, https://doi.org/10.1016/0040-1951(84)90176-8.

Liati, A., Gebauer, D., and Fanning, C.M., 2004, The age of ophiolitic rocks of the Hellenides (Vourinos, Pindos, Crete): First U-Pb ion microprobe (SHRIMP) zircon ages: Chemical Geology, v. 207, p. 171–188, https://doi.org/10.1016/j.chemgeo.2004.02.010.

Liu, Y.S., Hu, Z., Gao, S., Detlef, G., Xu, J., Gao, C., and Chen, H., 2008, In situ analysis of major and trace elements of anhydrous minerals by LA-ICP-MS without applying an internal standard: Chemical Geology, v. 257, p. 34–43, https://doi.org/10.1016/j.chemgeo.2008.08.004.

Ludwig, K.R., 2003, User's Manual for Isoplot 3.00: Berkeley Geochronology Center Special Publication 4, 74 p.

Lytwyn, J.N., and Casey, J.F., 1995, The geochemistry of postkinematic mafic dike swarms and subophiolitic metabasites, Pozantı-Karsantı ophiolite, Turkey: Evidence for ridge subduction: Geological Society of America Bulletin, v. 107, p. 830–850, https://doi.org/10.1130/0016-7606(1995)107<0830:TGOPMD>2.3.CO;2.

Ma, Q., Zheng, J., Griffin, W.L., Zhang, M., Tang, H., Su, Y., and Ping, X., 2012, Triassic adakitic rocks in an extensional setting (North China): Melts from the cratonic lower crust: Lithos, v. 149, p. 159–173, https://doi.org/10.1016/j.lithos.2012.04.017.

Mackintosh, P.W., and Robertson, A.H.F., 2013, Sedimentary and structural evidence for two-phase Upper Cretaceous and Eocene emplacement of the Tauride thrust sheets in central southern Turkey, *in* Robertson, A.H.F., Parlak, O., and Ünlügenç, U.C., eds., Geological Development of Anatolia and the Easternmost Mediterranean Region: Geological Society [London] Special Publication 372, p. 299–322.

Maffione, M., Thieulot, C., van Hinsbergen, D.J.J., Morris, A., Plumper, O., and Spakman, W., 2015, Dynamics of intraoceanic subduction initiation: 1. Oceanic detachment fault inversion and the formation of supra-subduction zone ophiolites: Geochemistry Geophysics Geosystems, v. 16, p. 1753–1770, https://doi.org/10.1002/2015GC005746.

Malpas, J., 1979, Two contrasting trondhjemite associations from transported ophiolites in western Newfoundland: Initial report, *in* Barker, F., ed., Trondhjemites, Dacites and Related Rocks: Amsterdam, Netherlands, Elsevier, p. 465–487, https://doi.org/10.1016/B978-0-444-41765-7.50020-4.

Maury, R.C., Lapierre, H., Bosch, D., Marcoux, J., Krystyn, L., Cotten, J., Bussy, F., Brunet, P., and Senebier, F., 2008, The alkaline intraplate volcanism of the Antalya nappes (Turkey): A Late Triassic remnant of the Neotethys: Bulletin de la Société Géologique de France, v. 179, p. 397–410, https://doi.org/10.2113/gssgfbull.179.4.397.

Monod, O., 1977, Récherches Géologique dans les Taurus Occidental au Aud de Beyşehir (Turquie) [thèse Doctorat]: Orsay, France, Université Paris-Sud, 450 p.

Morimoto, N., 1988, Nomenclature of pyroxenes: Mineralogical Magazine, v. 52, p. 535–550, https://doi.org/10.1180/minmag.1988.052.367.15.

Morris, A., and Robertson, A.H.F., 1993, Miocene remagnetization of carbonate platform and Antalya Complex units within the Isparta Angle, SW Turkey: Tectonophysics, v. 220, p. 243–266, https://doi.org/10.1016/0040-1951(93)90234-B.

Mukasa, S.B., and Ludden, J.N., 1987, Uranium-lead ages of plagiogranites from the Troodos ophiolite, Cyprus, and their tectonic significance: Geology, v. 15, p. 825–828, https://doi.org/10.1130/0091-7613(1987)15<825:UIAOPF>2.0.CO;2.

Okay, A.I., and Tüysüz, O., 1999, Tethyan sutures of northern Turkey, *in* Durand, B., Jolivet, L., Horvath, F., and Séranne, M., eds., The Mediterranean Basins: Tertiary Extension Within the Alpine Orogen: Geological Society [London] Special Publication 156, p. 475–515.

Okay, A.I., Harris, N.B.W., and Kelley, S., 1998, Exhumation of blueschists along a Tethyan suture in northwest Turkey: Tectonophysics, v. 285, p. 275–299, https://doi.org/10.1016/S0040-1951(97)00275-8.

Özgül, N., 1976, Torosların bazıtemel Jeoloji özellikleri: Bulletin of the Geological Society of Turkey, v. 19, p. 65–78.

Özgül, N., 1984, Stratigraphy and tectonic evolution of the central Taurides, *in* Tekeli, O., and Göncüoğlu, M.C., eds., Proceedings of the International Symposium on the Geology of the Taurus Belt: Ankara, Turkey, General Directorate of Mineral Research and Exploration (MTA), p. 77–90.

Özgül, N., and Arpat, E., 1973, Structural units of the Taurus orogenic belt and their continuation in the neighbouring regions: Bulletin of the Geological Society of Greece, v. 10, p. 155–164.

Paces, J.B., and Miller, J.D., 1993, Precise U-Pb ages of Duluth Complex and related mafic intrusions, northeastern Minnesota: Geochronological insights into physical, petrogenetic, paleomagnetic and tectonomagmatic processes associated with the 1.1 Ga Midcontinent rift system: Journal of Geophysical Research, v. 98, p. 13,997–14,013, https://doi.org/10.1029/93JB01159.

Parlak, O., 1996, Geochemistry and Geochronology of the Mersin Ophiolite within the Eastern Mediterranean Tectonic Frame [Ph.D. thesis]: Geneva, Switzerland, Department of Mineralogie, University of Geneva, 242 p.

Parlak, O., 2000, Geochemistry and significance of mafic dyke swarms in the Pozantı-Karsantı ophiolite (southern Turkey): Turkish Journal of Earth Sciences, v. 24, p. 29–38.

Parlak, O., 2016, The Tauride ophiolites of Anatolia (Turkey): A review: Journal of Earth Science, v. 27, p. 901–934, https://doi.org/10.1007/s12583-016-0679-3.

Parlak, O., and Delaloye, M., 1999, Precise $^{40}Ar/^{39}Ar$ ages from the metamorphic sole of the Mersin ophiolite (southern Turkey): Tectonophysics, v. 301, p. 145–158, https://doi.org/10.1016/S0040-1951(98)00222-4.

Parlak, O., and Robertson, A.H.F., 2004, Tectonic setting and evolution of the ophiolite-related Mersin mélange, southern Turkey: Its role in the tectonic-sedimentary setting of the Tethys in the Eastern Mediterranean region: Geological Magazine, v. 141, p. 257–286, https://doi.org/10.1017/S0016756804009094.

Parlak, O., Delaloye, M., and Bingöl, E., 1995a, Origin of subophiolitic metamorphic rocks beneath the Mersin ophiolite, southern Turkey: Ofioliti, v. 20, p. 97–110.

Parlak, O., Delaloye, M., and Bingöl, E., 1995b, Geochemistry of the volcanic rocks in the Mersin ophiolite (southern Turkey) and their tectonic significance in the Eastern Mediterranean geology, *in* Pişkin, Ö., Ergün, M., Savaşçın, M.Y., and Arcan, G.T., eds., Proceedings of International Earth Science Colloquium on the Aegean Region: İzmir, Turkey, Dokuz Eylül University, v. 2, p. 441–458.

Parlak, O., Höck, V., and Delaloye, M., 2000, Suprasubduction zone origin of the Pozanti-Karsanti ophiolite (southern Turkey) deduced from whole-rock and mineral chemistry of the gabbroic cumulates, *in* Bozkurt, E., Winchester, J.A., and Piper, J.D.A., eds., Tectonics and Magmatism in Turkey and the Surrounding Area: Geological Society [London] Special Publication 173, p. 219–234.

Parlak, O., Höck, V., Kozlu, H., and Delaloye, M., 2004, Oceanic crust generation in an island arc tectonic setting, SE Anatolian orogenic belt (Turkey): Geological Magazine, v. 141, p. 583–603, https://doi.org/10.1017/S0016756804009458.

Parlak, O., Yılmaz, H., and Boztuğ, D., 2006, Geochemistry and tectonic setting of the metamorphic sole rocks and isolated dykes from the Divriği ophiolite (Sivas, Turkey): Evidence for melt generation within an asthenospheric window prior to ophiolite emplacement: Turkish Journal of Earth Sciences, v. 15, p. 25–45.

Parlak, O., Rızaoğlu, T., Bağcı, U., Karaoğlan, F., and Höck, V., 2009, Tectonic significance of the geochemistry and petrology of ophiolites in southeast Anatolia, Turkey: Tectonophysics, v. 473, no. 1-2, p. 173–187.

Parlak, O., Karaoğlan, F., Rızaoğlu, T., Klötzli, U., Koller, F., and Billor, Z., 2013a, U-Pb and $^{40}Ar/^{39}Ar$ geochronology of the ophiolites and granitoids from the Tauride belt: Implications for the evolution of the Inner Tauride suture: Journal of Geodynamics, v. 65, p. 22–37, https://doi.org/10.1016/j.jog.2012.06.012.

Parlak, O., Çolakoğlu, A., Dönmez, C., Sayak, H., Yıldırım, N., Türkel, A., and Odabaşı, İ., 2013b, Geochemistry and tectonic significance of ophiolites along the İzmir–Ankara–Erzincan suture zone in northeastern Anatolia, *in* Robertson, A.H.F., Parlak, O., and Ünlügenç, U.C., eds., Geological Development of Anatolia and the Easternmost Mediterranean Region: Geological Society [London] Special Publication 372, p. 75–105.

Peacock, S.M., 1988, Inverted metamorphic gradients in the westernmost Cordillera, *in* Ernst, W.G., ed., Metamorphism and Crustal Evolution of the Western United States, Rubey Volume 7: Englewood Cliffs, New Jersey, Prentice-Hall, p. 953–975.

Pearce, J.A., 1982, Trace element characteristics of lavas from destructive plate boundaries, *in* Thorpe, R.S., ed., Andesites: Orogenic Andesites and Related Rocks: Chichester, UK, John Wiley and Sons, p. 525–548.

Pearce, J.A., 1983, Role of the sub-continental lithosphere in magma genesis at active continental margins, *in* Hawkesworth, C.J., and Norry, M.J., eds., Continental Basalts and Mantle Xenoliths: Nantwich, UK, Shiva, p. 230–249.

Pearce, J.A., 1996, A users guide to basalt discrimination diagrams, *in* Wyman, D.A., eds., Trace Element Geochemistry of Volcanic Rocks: Applications for Massive Sulphide Exploration: Geological Association of Canada Short Course Notes 12, p. 79–113.

Pearce, J.A., 2003, Supra-subduction zone ophiolites: The search for modern analogues, *in* Dilek, Y., and Newcomb, S., eds., Ophiolite Concept and the Evolution of Geological Thought: Geological Society of America Special Paper 373, p. 269–293, https://doi.org/10.1130/0-8137-2373-6.269.

Pearce, J.A., and Cann, J.R., 1973, Tectonic setting of basaltic volcanic rocks determined using trace element analysis: Earth and Planetary Science Letters, v. 19, p. 290–300, https://doi.org/10.1016/0012-821X(73)90129-5.

Pearce, J.A., Alabaster, T., Shelton, A.W., and Searle, M.P., 1981, The Oman ophiolite as a Cretaceous arc-basin complex: Evidence and implications: Philosophical Transactions of the Royal Society, ser. A, Mathematical, Physical and Engineering Sciences, v. 300, p. 299–317, https://doi.org/10.1098/rsta.1981.0066.

Pearce, J.A., Lippard, S.S., and Roberts, S., 1984, Characteristics and tectonic significance of suprasubduction zone ophiolites, *in* Kokelaar, B.P., and Howells, M.F., eds., Marginal Basin Geology: Volcanic and Associated Sedimentary and Tectonic Processes in Modern and Ancient Marginal Basins: Geological Society [London] Special Publication 16, p. 77–94.

Pearce, J.A., van der Laan, S.R., Arculus, R.J., Murton, B.J., Ishii, T., Peate, D.W., and Parkinson, I.J., 1992, Boninite and harzburgite from Leg 125 (Bonin-Mariana forearc): A case study of magma genesis during the initial stages of subduction, *in* Fryer, P., Pearce, J.A., Stokking, L.B., et al., Proceeding of the Ocean Drilling Program, Scientific Results Volume 125: College Station, Texas, Ocean Drilling Program, p. 623–659.

Pe-Piper, G., Tsıkouras, B., and Hatzıpanagıotou, K., 2004, Evolution of boninites and island-arc tholeiites in the Pindos ophiolite, Greece: Geological Magazine, v. 141, p. 455–469, https://doi.org/10.1017/S0016756804009215.

Pidgeon, R.T., 1992, Recrystallization of oscillatory-zoned zircon: some geochronological and petrological implications: Contributions to Mineralogy and Petrology, v. 110, p. 463-472.

Pidgeon, R.T., Nemchin, A.A., and Hitchen, G.J., 1998, Internal structures of zircons from Archaean granites from the Darling Range batholith: Implications for zircon stability and the interpretation of zircon U-Pb ages: Contributions to Mineralogy and Petrology, v. 132, p. 288–299, https://doi.org/10.1007/s004100050422.

Plunder, A., Agard, P., Chopin, C., Soret, M., Okay, A.İ., and Whitechurch, H., 2016, Metamorphic sole formation, emplacement and blueschist facies overprint: Early subduction dynamics witnessed by western Turkey ophiolites: Terra Nova, v. 28, p. 329–339, https://doi.org/10.1111/ter.12225.

Poisson, A., 1977, Recherches Géologiques dans les Taurides Occidentales (Turquie) [Ph.D. thesis]: Orsay, France, Université de Paris-Sud, 795 p.

Poisson, A., Yağmurlu, F., Bozcu, M., and Şentürk, M., 2003, New insights on the tectonic setting and evolution around the apex of the Isparta Angle (SW Turkey): Geological Journal, v. 38, p. 257–282, https://doi.org/10.1002/gj.955.

Polat, A., Casey, J.F., and Kerrich, R., 1996, Geochemical characteristics of accreted material beneath the Pozantı-Karsantı ophiolite, Turkey: Intra-oceanic detachment, assembly and obduction: Tectonophysics, v. 263, p. 249–276, https://doi.org/10.1016/S0040-1951(96)00026-1.

Pouchou, J.L., and Pichoir, F., 1984, A new model for quantitative X-ray microanalysis: Part I. Application of the analysis of homogeneous samples: La Recherche Aérospatiale, v. 3, p. 13–38.

Renne, P.R., Swisher, C.C., Deino, A.L., Karner, D.B., Owens, T.L., and De Paolo, D.L., 1998, Intercalibration of standards, absolute ages and uncertainties in $^{40}Ar/^{39}Ar$ dating: Chemical Geology, v. 145, p. 117–152, https://doi.org/10.1016/S0009-2541(97)00159-9.

Ricou, L.E., Marcoux, J., and Poisson, A., 1979, L'allochtonie des Bey Dağları orientaux, Reconstruction palinspastique

des Taurides occidentales: Bulletin de la Société Géologique de France, v. 21, p. 125–134, https://doi.org/10.2113/gssgfbull.S7-XXI.2.125.

Rioux, M., Bowring, S., Kelemen, P., Stacia, G., Dudás, F., and Miller, R., 2012, Rapid crustal accretion and magma assimilation in the Oman–U.A.E. ophiolite: High precision U-Pb zircon geochronology of the gabbroic crust: Journal of Geophysical Research–Solid Earth, v. 117, B07201, https://doi.org/10.1029/2012JB009273.

Rioux, M., Bowring, S., Kelemen, P., Stacia, G., Miller, R., and Dudás, F., 2013, Tectonic development of the Samail ophiolite: High-precision U-Pb zircon geochronology and Sm-Nd isotopic constraints on crustal growth and emplacement: Journal of Geophysical Research–Solid Earth, v. 118, p. 2085–2101, https://doi.org/10.1002/jgrb.50139.

Rioux, M., Garber, J., Bauer, A., Bowring, S., Searle, M., Kelemen, P., and Hacker, B., 2016, Synchronous formation of the metamorphic sole and igneous crust of the Semail ophiolite: New constraints on the tectonic evolution during ophiolite formation from high-precision U-Pb zircon geochronology: Earth and Planetary Science Letters, v. 451, p. 185–195, https://doi.org/10.1016/j.epsl.2016.06.051.

Rızaoğlu, T., Parlak, O., Höck, V., and İşler, F., 2006, Nature and significance of Late Cretaceous ophiolitic rocks and its relation to the Baskil granitoid in Elazığ region, SE Turkey, *in* Robertson, A.H.F., and Mountrakis, D., eds., Tectonic Development of the Eastern Mediterranean Region: Geological Society [London] Special Publication 260, p. 327–350.

Rizvanova, N.G., Lenchenkov, O.A., and Belous, A.E., 2000, Zircon reaction and stability of the U-Pb isotope system during the interaction with carbonate fluid: Experimental hydrothermal study: Contributions to Mineralogy and Petrology, v. 139, p. 101–114, https://doi.org/10.1007/s004100050576.

Roberts, N.M.W., Thomas, R.J., and Jacobs, J., 2016, Geochronological constraints on the metamorphic sole of the Semail ophiolite in the United Arab Emirates: Geoscience Frontiers, v. 7, p. 609–619, https://doi.org/10.1016/j.gsf.2015.12.003.

Robertson, A.H.F., 2002, Overview of the genesis and emplacement of Mesozoic ophiolites in the Eastern Mediterranean Tethyan region: Lithos, v. 65, no. 1-2, p. 1–67, https://doi.org/10.1016/S0024-4937(02)00160-3.

Robertson, A.H.F., 2004, Development of concepts concerning the genesis and emplacement of Tethyan ophiolites in the Eastern Mediterranean and Oman regions: Earth-Science Reviews, v. 66, no. 3-4, p. 331–387, https://doi.org/10.1016/j.earscirev.2004.01.005.

Robertson, A.H.F., and Dixon, J.A., 1984, Introduction: Aspects of the geological evolution of the Eastern Mediterranean, *in* Dixon, J.A., and Robertson, A.H.F., eds., The Geological Evolution of the Eastern Mediterranean: Geological Society [London] Special Publication 17, p. 1–74.

Robertson, A.H.F., and Waldron, J., 1990, Geochemistry and tectonic setting of Late Triassic and Late Jurassic–Early Cretaceous basaltic extrusives from the Antalya Complex, SW Turkey, *in* Savaşçın, M.Y., and Eronat, A.H., eds., Proceedings of International Earth Science Congress on Aegean Regions, Volume 2: İzmir, Turkey, Dokuz Eylül University, p. 279–299.

Robertson, A.H.F., Poisson, A., and Akıncı, Ö., 2003, Developments in research concerning Mesozoic–Tertiary Tethys and neotectonics in the Isparta Angle, SW Turkey: Geological Journal, v. 38, p. 195–234, https://doi.org/10.1002/gj.953.

Robertson, A.H.F., Parlak, O., and Ustaömer, T., 2009, Mélange genesis and ophiolite emplacement related to subduction of the northern margin of the Tauride-Anatolide continent, central and western Turkey, *in* van Hinsbergen, D.J.J., Edwards, M.A., and Govers, R., eds., Collision and Collapse at the Africa-Arabia-Eurasia Subduction Zone: Geological Society [London] Special Publication 311, p. 9–66.

Robertson, A.H.F., Parlak, O., Ustaömer, T., Taslı, K., İnan, N., Dumitrica, P., and Karaoğlan, F., 2013, Subduction, ophiolites genesis and collision history of Tethys adjacent to the Eurasian continental margin: New evidence from the Eastern Pontides, Turkey: Geodinamica Acta, v. 26, no. 3-4, p. 230–293, https://doi.org/10.1080/09853111.2013.877240.

Robertson, A.H.F., Parlak, O., Yıldırım, N., Dumitrica, P., and Taslı, K., 2016, Late Triassic rifting and Jurassic–Cretaceous passive margin development of the southern Neotethys: Evidence from the Adıyaman area, SE Turkey: International Journal of Earth Sciences, v. 105, p. 167–201, https://doi.org/10.1007/s00531-015-1176-0.

Rojay, B., Yalınız, M.K., and Altıner, D., 2001, Tectonic implications of some Cretaceous pillow basalts from the North Anatolian ophiolitic mélange (Central Anatolia-Turkey) to the evolution of Neotethys: Turkish Journal of Earth Sciences, v. 10, p. 93–102.

Saccani, E., and Photiades, A., 2005, Petrogenesis and tectonomagmatic significance of volcanic and subvolcanic rocks in the Albanide-Hellenide ophiolitic mélanges: The Island Arc, v. 14, p. 494–516, https://doi.org/10.1111/j.1440-1738.2005.00480.x.

Sarıfakıoğlu, E., Dilek, Y., and Uysal, İ., 2012, The Petrogenesis and Geodynamic Significance of Bahçe (Osmaniye) Ophiolite, *in* Proceedings of the 5th Geochemistry Symposium, 23-25 May 2009, Denizli, Turkey, Pamukkale University, p. 112–113.

Schmidt, M.W., 1992, Amphibole composition in tonalite as a function of pressure—An experimental calibration of the al-in-hornblende barometer: Contributions to Mineralogy and Petrology, v. 110, no. 2-3, p. 304–310, https://doi.org/10.1007/BF00310745.

Searle, M., and Cox, J., 1999, Tectonic setting, origin and obduction of the Oman ophiolite: Geological Society of America Bulletin, v. 111, p. 104–122, https://doi.org/10.1130/0016-7606(1999)111<0104:TSOAOO>2.3.CO;2.

Searle, M., and Cox, J., 2002, Subduction zone metamorphism during formation and emplacement of the Semail ophiolite in the Oman Mountains: Geological Magazine, v. 139, p. 241–255, https://doi.org/10.1017/S0016756802006532.

Searle, M.P., and Malpas, J., 1980, The structure and metamorphism of rocks beneath the Semail ophiolite of Oman and their significance in ophiolite obduction: Transactions of the Royal Society of Edinburgh–Earth Sciences, v. 71, p. 247–262, https://doi.org/10.1017/S0263593300013614.

Searle, M.P., and Malpas, J., 1982, Petrochemistry and origin of sub-ophiolitic metamorphic and related rocks in the Oman Mountains: Journal of the Geological Society [London], v. 139, p. 235–248, https://doi.org/10.1144/gsjgs.139.3.0235.

Searle, M.P., Waters, D.J., Garber, J.M., Rioux, M., Cherry, A.G., and Ambrose, T.K., 2015, Structure and metamorphism beneath the obducting Oman ophiolite: Evidence from the Bani Hamid granulites, northern Oman mountains: Geosphere, v. 11, no. 6, p. 1812–1836, https://doi.org/10.1130/GES01199.1.

Şengör, A.M.C., and Yılmaz, Y., 1981, Tethyan evolution of Turkey: A plate tectonic approach: Tectonophysics, v. 75, p. 181–241, https://doi.org/10.1016/0040-1951(81)90275-4.

Shervais, J.W., 2001, Birth, death, and resurrection: The life cycle of suprasubduction zone ophiolites: Geochemistry Geophysics Geosystems, v. 2, 1010, https://doi.org/10.1029/2000GC000080.

Sláma, J., Košler, J., Condon, D.J., Crowley, J.L., Gerdes, A., Hanchar, J.M., et al., 2008, Plešovice zircon—A new natural reference material for U-Pb and Hf isotopic microanalysis: Chemical Geology, v. 249, p. 1–35, https://doi.org/10.1016/j.chemgeo.2007.11.005.

Spray, J.G., 1984, Possible causes and consequences of upper mantle decoupling and ophiolite displacement, *in* Gass, I.G., Lippard, S.J., and Shelton, A.W., eds., Ophiolites and Oceanic Lithosphere: Geological Society [London] Special Publication 13, p. 255–268.

Stern, R.J., 2004, Subduction initiation: Spontaneous and induced: Earth and Planetary Science Letters, v. 226, p. 275–292, https://doi.org/10.1016/S0012-821X(04)00498-4.

Stern, R.J., and Bloomer, S.H., 1992, Subduction zone infancy: Examples from the Eocene Izu-Bonin-Mariana and Jurassic California: Geological Society of America Bulletin, v. 104, p. 1621–1636, https://doi.org/10.1130/0016-7606(1992)104<1621:SZIEFT>2.3.CO;2.

Stern, R.J., Reagan, M., Ishizuka, O., Ohara, Y., and Whattam, S., 2012, To understand subduction initiation, study forearc crust: To understand forearc crust, study ophiolites: Lithosphere, v. 4, p. 469–483, https://doi.org/10.1130/L183.1.

Su, B.X., Chen, C., Pang, K.N., Sakyi, P.A., Uysal, İ., Avcı, E., Liu, X., and Zhang, P.F., 2018, Melt penetration in oceanic lithosphere: Li isotope records from the Pozantı-Karsantı ophiolites in southern Turkey: Journal of Petrology, v. 59, p. 191–205, https://doi.org/10.1093/petrology/egy023.

Sun, S.S., and McDonough, W.F., 1989, Chemical and isotopic systematics of oceanic basalts: Implications for mantle composition and processes, *in* Saunders, A.D., and Norry, M.J., eds., Magmatism in the Ocean Basins: Geological Society [London] Special Publications 42, p. 313–345.

Taylor, B., 1992, Rifting and the volcanic-tectonic evolution of the Izu-Bonin-Mariana arc, *in* Taylor, B., Fujioka, K., et al., Proceedings of the Ocean Drilling Program, Scientific Results Volume 126: College Station, Texas, Ocean Drilling Program, p. 627–651.

Teipel, U., Eichhorn, R., Loth, G., Rohrmfuller, J., Hfoll, R., and Kennedy, A., 2004, U-Pb SHRIMP and Nd isotopic data from the western Bohemian Massif (Bayerischer Wald, Germany): Implications for Upper Vendian and Lower Ordovician magmatism: International Journal of Earth Sciences, v. 93, p. 782–801, https://doi.org/10.1007/s00531-004-0419-2.

Thompson, G., 1991, Metamorphic and hydrothermal processes: Basalt-seawater interactions, *in* Floyd, P.A., ed., Oceanic Basalts: Glasgow, UK, Blackie, p. 148–173.

Thuizat, R., Whitechurch, H., Montigny, R., and Juteatu, T., 1981, K-Ar dating of some infra-ophiolitic metamorphic soles from the Eastern Mediterranean: New evidence for oceanic thrusting before obduction: Earth and Planetary Science Letters, v. 52, p. 302–310, https://doi.org/10.1016/0012-821X(81)90185-0.

Tomaschek, F., Kennedy, A.K., Villa, I.M., and Ballhaus, C., 2003, Zircons from Syros, Cyclades, Greece—Recrystallization and mobilization of zircon during high-pressure metamorphism: Journal of Petrology, v. 44, p. 1977–2002, https://doi.org/10.1093/petrology/egg067.

Topuz, G., Göçmengil, G., Rolland, Y., Çelik, Ö.F., Zack, T., and Schmitt, A.K., 2013, Jurassic accretionary and ophiolite from northeast Turkey: No evidence for the Cimmerian continental ribbon: Geology, v. 41, p. 255–258, https://doi.org/10.1130/G33577.1.

van Hinsbergen, D.J.J., Peters, K., Maffione, M., Spakman, W., Guilmette, C., Thieulot, C., Plümper, O., Gürer, D., Brouwer, F.M., Aldanmaz, E., and Kaymakcı, N., 2015, Dynamics of intraoceanic subduction initiation: 2. Suprasubduction zone ophiolite formation and metamorphic sole exhumation in context of absolute plate motions: Geochemistry Geophysics Geosystems, v. 16, p. 1771–1785, https://doi.org/10.1002/2015GC005745.

van Hinsbergen, D.J.J., Maffione, M., Plunder, A., Kaymakçı, N., Ganerod, M., Hendriks, B.W.H., Corfu, F., Gürer, D., de Gelder, G.I.N.O., Peters, K., McPhee, P.J., Brouwer, F.M., Advokaat, E.L., and Vissers, R.L.M., 2016, Tectonic evolution and paleogeography of the Kırşehir block and the Central Anatolian ophiolites, Turkey: Tectonics, v. 35, p. 983–1014, https://doi.org/10.1002/2015TC004018.

Vanko, D.A., and Laverne, C., 1998, Hydrothermal anorthitization of plagioclase within the magmatic/hydrothermal transition at mid-ocean ridges: Examples from deep sheeted dikes (Hole 504B, Costa Rica Rift) and a sheeted dike root zone (Oman ophiolite): Earth and Planetary Science Letters, v. 162, no. 1-4, p. 27–43, https://doi.org/10.1016/S0012-821X(98)00155-1.

Varol, E., Bedi, Y., Tekin, U.K., and Uzunçimen, S., 2011, Geochemical and petrological characteristics of Late Triassic basic volcanic rocks from the Koçali Complex, SE Turkey: Implications for the Triassic evolution of Southern Tethys: Ofioliti, v. 36, p. 101–115.

Vergili, Ö., and Parlak, O., 2005, Geochemistry and tectonic setting of metamorphic sole rocks and mafic dykes from the Pınarbaşı (Kayseri) ophiolite, Central Anatolia: Ofioliti, v. 30, p. 37–52.

Wakabayashi, J., and Dilek, Y., 2000, Spatial and temporal relations between ophiolites and their subophiolitic soles: A test of models of forearc ophiolite genesis, *in*

Dilek, Y., Moores, E.M., Elthon, D., and Nicolas, A., eds., Ophiolites and Oceanic Crust: New Insights from Field Studies and the Ocean Drilling Program: Geological Society of America Special Paper 349, p. 53–64, https://doi.org/10.1130/0-8137-2349-3.53.

Wakabayashi, J., and Dilek, Y., 2003, What constitutes emplacement of an ophiolite?: Mechanisms and relationship to subduction initiation and formation of metamorphic soles, *in* Dilek, Y., and Robinson, P.T., eds., Ophiolites in Earth History: Geological Society [London] Special Publication 218, p. 427–447.

Wallin, E.T., and Metcalf, R.V., 1998, Supra-subduction zone ophiolites formed in an extensional forearc: Trinity terrane, Klamath Mountains, California: The Journal of Geology, v. 106, p. 591–608, https://doi.org/10.1086/516044.

Warren, C.J., Parrish, R.R., Waters, D.J., and Searle, M.P., 2005, Dating the geologic history of Oman's Semail ophiolite: Insights from U-Pb geochronology: Contributions to Mineralogy and Petrology, v. 150, p. 403–422, https://doi.org/10.1007/s00410-005-0028-5.

Wiedenbeck, M., Alle, P., Corfu, F., Griffin, W.L., Meier, M., Oberli, F., Von Quadt, A., Roddick, J.C., and Spiegel, W., 1995, Three natural zircon standards for U-Th-Pb, Lu-Hf, trace element and REE analyses: Geostandards Newsletter, v. 19, p. 1–23, https://doi.org/10.1111/j.1751-908X.1995.tb00147.x.

Williams, H., and Smyth, W.R., 1973, Metamorphic aureoles beneath ophiolite suites and Alpine peridotites: Tectonic implications with west Newfoundland examples: American Journal of Science, v. 273, p. 594–621, https://doi.org/10.2475/ajs.273.7.594.

Wood, D.A., Joron, J.L., and Treuil, M., 1979, A reappraisal of the use of trace elements to classify and discriminate between magma series erupted in different tectonic settings: Earth and Planetary Science Letters, v. 45, p. 326–336, https://doi.org/10.1016/0012-821X(79)90133-X.

Wu, Y.B., and Zheng, Y.F., 2004, Genesis of zircon and its constraints on interpretation of U-Pb age: Chinese Science Bulletin, v. 49, p. 1554–1569, https://doi.org/10.1007/BF03184122.

Yalınız, K.M., Floyd, P., and Göncüoğlu, M.C., 1996, Supra-subduction zone ophiolites of Central Anatolia: Geochemical evidence from the Sarikaraman ophiolite, Aksaray, Turkey: Mineralogical Magazine, v. 60, p. 697–710, https://doi.org/10.1180/minmag.1996.060.402.01.

Yalınız, K.M., Floyd, P.A., and Göncüoğlu, M.C., 2000, Geochemistry of volcanic rocks from the Çiçekdağ ophiolite, Central Anatolia, Turkey, and their inferred tectonic setting within the northern branch of the Neotethyan Ocean, *in* Bozkurt, E., Winchester, J.A., and Piper, J.D.A., eds., Tectonics and Magmatism in Turkey and the Surrounding Area: Geological Society [London] Special Publication 173, p. 203–218.

Yogodzinski, G.M., Volynets, O.N., Koloskov, A.V., Seliverstov, N.I., and Matvenkov, V.V., 1994, Magnesian andesites and the subduction component in strongly calc-alkaline series at Piip volcano, far western Aleutians: Journal of Petrology, v. 35, p. 163–204, https://doi.org/10.1093/petrology/35.1.163.

Science Editor: Bradley S. Singer
Associate Editor: Erdin Bozkurt

Manuscript Received 18 June 2018
Revised Manuscript Received 27 November 2018
Manuscript Accepted 7 February 2019

Printed in the USA